DOI: 10.1534/genetics.109.107508

Centromere Replication Timing Determines Different Forms of Genomic Instability in *Saccharomyces cerevisiae* Checkpoint Mutants During Replication Stress

Wenyi Feng,* Jeff Bachant,† David Collingwood,‡ M. K. Raghuraman* and Bonita J. Brewer*,[1]

**Department of Genome Sciences and* ‡*Department of Mathematics, University of Washington, Seattle, Washington 98195 and* †*Department of Cell Biology and Neuroscience, University of California, Riverside, California 92521*

Manuscript received July 17, 2009
Accepted for publication September 23, 2009

ABSTRACT

Yeast replication checkpoint mutants lose viability following transient exposure to hydroxyurea, a replication-impeding drug. In an effort to understand the basis for this lethality, we discovered that different events are responsible for inviability in checkpoint-deficient cells harboring mutations in the *mec1* and *rad53* genes. By monitoring genomewide replication dynamics of cells exposed to hydroxyurea, we show that cells with a checkpoint deficient allele of *RAD53*, *rad53K227A*, fail to duplicate centromeres. Following removal of the drug, however, *rad53K227A* cells recover substantial DNA replication, including replication through centromeres. Despite this recovery, the *rad53K227A* mutant fails to achieve biorientation of sister centromeres during recovery from hydroxyurea, leading to secondary activation of the spindle assembly checkpoint (SAC), aneuploidy, and lethal chromosome segregation errors. We demonstrate that cell lethality from this segregation defect could be partially remedied by reinforcing bipolar attachment. In contrast, cells with the *mec1-1 sml1-1* mutations suffer from severely impaired replication resumption upon removal of hydroxyurea. *mec1-1 sml1-1* cells can, however, duplicate at least some of their centromeres and achieve bipolar attachment, leading to abortive segregation and fragmentation of incompletely replicated chromosomes. Our results highlight the importance of replicating yeast centromeres early and reveal different mechanisms of cell death due to differences in replication fork progression.

CENTROMERES have long been known to be one of the earliest regions of the budding yeast genome to replicate during S phase (McCarroll and Fangman 1988). However, the biological significance of early replication of centromeres remains speculative, partly owing to the lack of mutants showing altered or delayed timing of centromere replication. During our investigation of chromosome replication dynamics during nucleotide shortage brought upon by the treatment with hydroxyurea (HU), we discovered that problems with centromere replication can lead to fundamentally different forms of genome instability.

The two mutations that exhibit interesting centromere replication phenotypes are in the genes encoding two essential protein kinases, Mec1 and Rad53, which play pivotal roles in the cellular response to DNA damaging agents as well as in cell cycle arrest in response to HU (Branzei and Foiani 2006; Tourriere and Pasero 2007). Mutations in the kinase domains of Mec1 and Rad53 render the proteins checkpoint deficient and cause the cells carrying such mutations to be hypersensitive to HU. Because Mec1 is an upstream effector of Rad53 in the replication checkpoint pathway, checkpoint-deficient alleles of the two genes are thought to lead to similar phenotypes in response to replication impediments. When *rad53* cells encounter HU during S phase, they fail to slow the temporal program of origin firing, expose large regions of single-stranded DNA (ssDNA) at effectively all origins, and elongate their spindles, a phenotype that indicates that the cells are attempting premature chromosome partitioning (Allen *et al.* 1994; Weinert *et al.* 1994; Desany *et al.* 1998; Santocanale and Diffley 1998; Sogo *et al.* 2002; Feng *et al.* 2006). Similarly, *mec1* cells have also been shown to initiate precocious segregation of unreplicated chromosomes upon exposure to HU (Weinert *et al.* 1994; Sanchez *et al.* 1996). Even after the removal of HU, both *mec1* and *rad53* cells show considerable reduction in their ability to produce progeny. However, the reason for inviability after HU exposure is ill defined. We reasoned that understanding the molecular basis of cell death would help elucidate the role of checkpoint control in DNA replication and cell cycle regulation and in the maintenance of genome integrity.

Previous reports indicated that following transient exposure to HU, *rad53* checkpoint-deficient cells are

Supporting information is available online at http://www.genetics.org/cgi/content/full/genetics.109.107508/DC1.

[1]*Corresponding author:* Department of Genome Sciences, University of Washington, Box 355065 Foege Bldg., Room S041, 1705 NE Pacific St., Seattle, WA 98195. E-mail: bbrewer@gs.washington.edu

unable to complete DNA replication, which in turn was thought to constitute the primary reason for the loss of viability (Desany *et al.* 1998; Lopes *et al.* 2001). This conclusion was corroborated by the observation that delaying premature chromosome segregation by inhibiting microtubule assembly (via nocodazole treatment) following HU exposure was unable to improve the viability of *rad53* cells (Desany *et al.* 1998). Together, these studies suggested that incomplete replication rather than premature chromosome segregation *per se* was the major reason for loss of viability in both *rad53* and *mec1* cells, following treatment with HU. By flow cytometric measurements it appeared that *rad53* cells were able to replicate slowly a significant amount of genomic DNA following transient (30–60 min) exposure to HU, but that these chromosomes did not enter pulse field gels (Desany *et al.* 1998). The authors proposed that the DNA synthesized by *rad53* cells must contain gaps, branches, or other structures that retard the mobility of chromosomal DNA in the pulse field gels. The presence of putative abnormal replication intermediates was later revealed by two-dimensional gel electrophoresis and by electron microscopy (Lopes *et al.* 2001; Sogo *et al.* 2002).

Intrigued by the results of Desany *et al.* (1998), we decided to ask where in the genome DNA replication occurred during recovery from HU—in particular, whether forks established during HU treatment were able to resume or whether replication was occurring from unfired origins. By addressing this question, we hoped to identify what precisely was the defect, if any, in DNA replication during the recovery phase from HU in cells lacking the checkpoint function.

In this study, we examine the cellular responses of two checkpoint-deficient mutants, *mec1-1 sml1-1* and *rad53K227A* (Weinert *et al.* 1994; Sogo *et al.* 2002), upon exposure to HU during the initiation of S phase and during recovery after HU is removed. We chose the *mec1-1 sml1-1* strain for our studies because it is in an isogenic background (A364a) as the *rad53K227A* mutant that we have previously studied. The *mec1-1* allele is phenotypically identical to a *mec1* null allele and it requires the *sml1-1* mutation for viability (Zhao *et al.* 1998; Basrai *et al.* 1999). In contrast, the *rad53K227A* mutation (Feng *et al.* 2006) is not lethal and the strain harboring this mutation does not contain the *sml1-1* allele (data not shown). Through the usage of these specific mutations in the checkpoint pathway, we observed that the *mec1-1 sml1-1* and *rad53K227A* cells, upon exposure to HU, lose viability through distinct mechanisms that arise from differences in centromere replication in the two mutants. We further demonstrate that the extent to which the two mutants recover DNA synthesis upon the removal of HU also differs. Our study reveals the importance of early replication of centromeres and underscores the involvement of the replication checkpoint pathway in the establishment of chromosome biorientation.

MATERIALS AND METHODS

Yeast strains and media: Yeast strains used in this study are listed in supporting information, Table S2. Cells were grown at 30° in synthetic complete medium unless otherwise indicated. α-Factor was used at 200 nm for *bar1* strains and 3 μm for *BAR1* strains. Pronase was used at 25 μg/ml and 300 μg/ml for *bar1* and *BAR1* strains, respectively, to remove α-factor from the culture medium. HU was added at 200 mm and nocodazole was used at 15 μg/ml.

Measurement of cell viability by colony formation assay: Cells synchronized in G1 by α-factor treatment were released into medium containing 200 mm HU or in combination with 15 μg/ml nocodazole as detailed in the main text. Aliquots of 100 μl were removed for serial dilutions in ice-cold minimal medium lacking a nitrogen source. The cell suspension of the appropriate concentration was sonicated briefly before plating aliquots in triplicate on solid medium. The plates were incubated at 30° for 2–3 days before colonies were counted and analyzed.

Contour-clamped homogeneous electric field gel electrophoresis and Southern blotting: Contour-clamped homogeneous electric field (CHEF) gel analysis was performed as described previously (van Brabant *et al.* 2001). Electrophoresis was conducted at 14° for 25 hr with a switch time ramped from 60 to 120 sec at 200 V. The Chr IX probe was amplified from genomic DNA with primers of the following sequences: forward, 5′-CTATGACGAGGGCGAAGAAG-3′; reverse, 5′-ATTTCACAGGGCCAGACACG-3′. Southern blotting was performed according to standard procedures.

Flow cytometry: Cells were collected and mixed with 0.1% NaN_3, followed by fixing with 70% ethanol. Flow cytometry was performed using standard procedures after staining the cells with Sytox Green (Molecular Probes) and the data were analyzed with CellQuest software (Becton-Dickinson).

Chromosome biorientation assay: Cells carrying the *CEN4-GFP* tag and the *cdc23-1* mutation were blocked in G1 with α-factor and released into YPD medium at 35° (to block cells at the metaphase/anaphase transition by inactivating the Cdc23 protein) in the presence or absence of 200 mm HU. After 1 hr, cells were allowed to recover in fresh medium lacking HU at 35°. At the indicated times, samples were evaluated for the percentage of cells with two separated *CEN4-GFP* foci, indicative of successful biorientation at the *cdc23* block.

Indirect end labeling: Yeast chromosomes embedded in agarose gels were prepared as previously described (van Brabant *et al.* 2001). A detailed protocol for in-gel restriction digestion can be found at http://fangman-brewer.genetics.washington.edu/fork-D.html. The digested agarose plugs were then placed in wells of a 0.4% agarose gel (without ethidium bromide) and electrophoresed at 1 V/cm for 26 hr at room temperature. Standard Southern blotting techniques were used. The primer sequences for the *DSF2* probe are: DSF2-F, 5′-TTTCATTACCTCCAACGCCA-3′; DSF2-R, 5′-TTTCGGACCTTGTTTCATGT-3′. The *TRP1* probe was isolated as a *Hin*dIII fragment from plasmid pTA-DIR (M. K. Raghuraman, unpublished results.).

Genomic ssDNA mapping: ssDNA analysis on *rad53* and *mec1 sml1* cells was performed as previously described (Feng *et al.* 2006, 2007).

Density transfer: Dense-isotope substitution experiments were performed essentially as described earlier (McCarroll and Fangman 1988; Raghuraman *et al.* 2001) with modifications. A detailed protocol can be found at http://fangman-brewer.genetics.washington.edu/density_transfer.html. Thirty minutes prior to the release from α-factor the culture was transferred to isotopically light medium to equilibrate nucleotide pools. HU was added at 200 mm just prior to pronase addition. After 1

(for *rad53* and *mec1 sml1* cells) or 2 [for wild-type (WT) cells] hr, cells were filtered to remove HU and allowed to recover in fresh medium without HU. Samples were collected at the times indicated in the figure legends and genomic DNA was extracted followed by fractionation after ultracentrifugation in a CsCl density gradient. An aliquot of each gradient fraction was slot blotted, followed by hybridization with centromere DNA probes (*CEN2* and *CEN4*) or a whole–genomic DNA probe to identify the unreplicated (HH) DNA and replicated (HL) DNA. The *CEN2* fragment was amplified from genomic DNA with the following primers: forward, 5′-TAGTCTATCAGCCTCCGAAG-3′; reverse, 5′-GTA GGT GCCAGTTGAATAGC-3′. The *CEN4* fragment was excised as a *Xho*I-*Spe*I restriction fragment from the plasmid YCpG. EDam^{td} (M. K. Raghuraman, unpublished results). For microarray analysis, those fractions containing HH and HL DNA identified by slot blotting and hybridization with a genomic DNA probe were pooled, respectively. The HH and HL DNA for each timed sample were differentially labeled with cyanine (Cy3 or Cy5)-conjugated dUTP (Perkin Elmer) as described by the Brown laboratory (http://cmgm.stanford.edu/pbrown/protocols/4_genomic.html) followed by purification through a Sephadex G-50 column and ethanol precipitation for microarray hybridization.

Microarray hybridization and analysis: See File S2.

RESULTS

Extent of replication fork progression in HU inferred from ssDNA profiles: Treatment of checkpoint-deficient *rad53K227A* cells (henceforth referred to as *rad53* cells) with HU during a synchronized S phase generates regions of ssDNA restricted to the immediate vicinity of virtually all replication origins in the yeast genome (Feng *et al.* 2006, 2007). The colocalization of ssDNA with origins suggests that replication forks are unable to progress very far into adjacent regions before they become arrested. To assess whether the accumulation of ssDNA at origins is unique to the *rad53* mutation, we analyzed a *mec1-1 sml1-1* (henceforth referred to as *mec1 sml1*) checkpoint deficient mutant under similar conditions.

When we released *mec1 sml1* cells from a G1 arrest into HU for 1 hr, ssDNA also appeared at virtually all replication origins in the genome. However the peaks of ssDNA in *mec1 sml1* cells, though significantly above background, were lower, broader, and often "split" in comparison to those in *rad53K227A* cells (data from Feng *et al.* 2006; Figure 1 and Figure S1), suggesting that replication forks in *mec1 sml1* cells were able to proceed further than were forks in *rad53* cells. While the majority of centromeres in *rad53* cells are located in troughs between ssDNA peaks, in *mec1 sml1* cells, ssDNA extended into some centromeric regions (such as Chr VII, Figure 1, open block arrow). This observation prompted us to investigate whether centromere duplication during HU treatment differs between these two mutants.

Centromere replication in HU: We examined the extent of centromere replication in *rad53* and *mec1 sml1* cells during exposure to HU using a density transfer

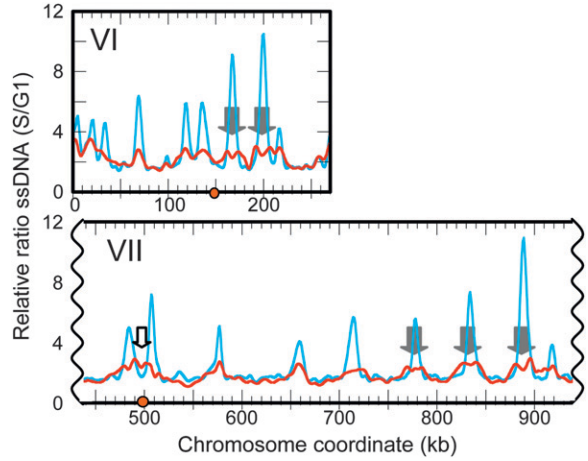

Figure 1.—Genomic ssDNA mapping reveals more extensive migration of replication forks in *mec1 sml1* (yMP10913) cells than in *rad53* (WFY34) cells. Cells were released from G1 arrest to enter S phase in the presence of 200 mM HU. Samples were collected at 0 (α-factor arrested) and 1 hr (S phase) and DNA from the two samples was isolated, differentially labeled with Cy-conjugated dUTPs without the denaturation of template DNA (to limit synthesis to the single-stranded portions of the genome; details in Feng *et al.* 2007), and cohybridized to a microarray to obtain the relative ratio of ssDNA in the S phase sample to that in the G1 control sample (S/G1) at any region of the genome. The ratio of ssDNA for *rad53* (cyan) and *mec1 sml1* (red) for chromosome VI and a portion of VII are shown. Gray block arrows mark "split peaks" and the open block arrow marks ssDNA near *CEN7*. Orange dots indicate centromere locations. See Figure S1 for all 16 chromosomes.

method (Figure 2A). Following *Eco*RI digestion, unreplicated (HH) and replicated (HL) genomic DNA were hybridized with probes to detect the *Eco*RI fragments that contained *CEN2* (4.078 kb, 65.1% A+T) and *CEN4* (5.778 kb, 63.5% A+T) (see materials and methods; Figure 2A). These centromeres differ in the distance to the nearest potential origin of replication or autonomously replicating sequence (ARS): *CEN2* is ~500 bp from *ARS208* and *CEN4* is 13.7 kb from *ARS1* (Figure 2B). Surprisingly, neither of the fragments in the *rad53* or the *mec1 sml1* sample showed any DNA of fully hybrid density (HL) at T1hr in HU (Figure 2C). However, the profile of *CEN2* in *mec1 sml1* cells at T1hr is slightly broader and shifted more to the HL position than that at T0 (Figure 2C), consistent with partial replication. No such shift is observed for either centromere in the *rad53* sample. Given the presence of ssDNA in the sample, the actual amount of replication that had occurred at *CEN2* may be underrepresented, as indicated by the observation that filling in the ssDNA gaps by *in vitro* synthesis increased the shift to the HL position in the *mec1 CEN2* but not *CEN4* fragment (Figure S2). From the extent of the shift we estimate that replication forks from *ARS208* on the *CEN2* fragments synthesized an average of <1 kb. On the basis of the calculated distances between each of the 16 centromeres and their

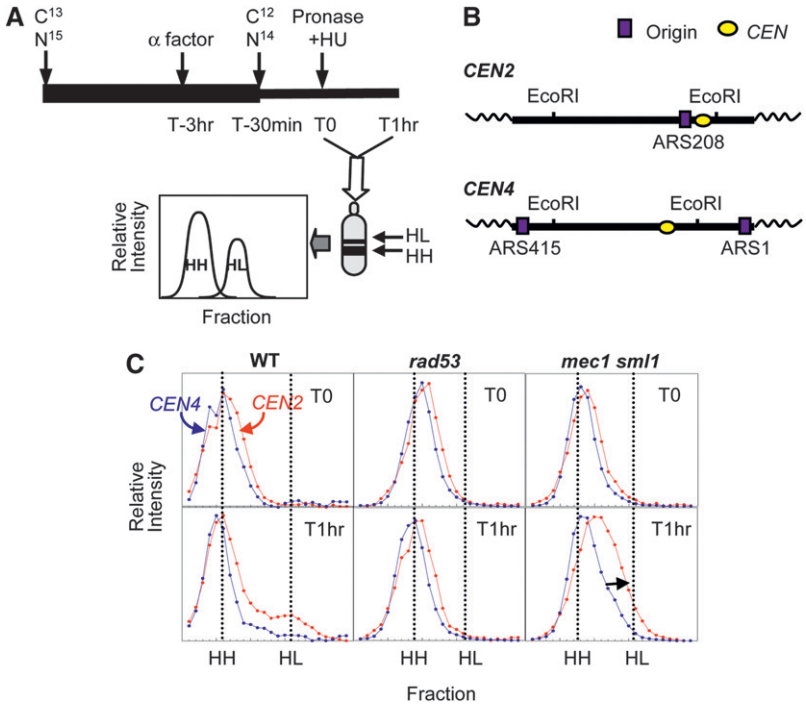

FIGURE 2.—Differences in centromere replication in *mec1 sml1* (WFY73) and *rad53* (WFY34) cells in HU. HM14-3a cells were used as a WT control. (A) Experimental scheme for density transfer and subsequent analyses. Cells were propagated in isotopically dense (^{13}C and ^{15}N) medium for at least eight generations prior to G1 arrest. At 30 min prior to release into S phase (time = T-30 min), cells were switched to light medium (^{12}C and ^{14}N) to allow nucleotide pools to equilibrate. At time 0 (T0), cells were released into S phase in the presence of 200 mM HU. The culture was harvested an hour later (T1hr). DNA was extracted, digested with *Eco*RI and subjected to equilibrium centrifugation in CsCl gradients to separate HH (unreplicated) and HL (replicated) DNA. The resulting gradients were fractionated and each fraction slot blotted onto nylon membranes to allow hybridization with specific DNA probes. (B) *CEN2* and *CEN4* locations in relation to their neighboring origins on their respective *Eco*RI fragments (not drawn to scale). (C) Relative amounts of replication of the *Eco*RI fragments containing *CEN4* (blue) and *CEN2* (red), for *rad53* and *mec1 sml1*. The spreading of the HH peak toward the position of hybrid DNA (HL) is indicated by a black arrow.

nearest ARSs (using a compiled origin list by Nieduszynski, http://www.oridb.org) only two centromeres (*CEN3* and *CEN12*) are closer to an ARS than *CEN2* is (Table S1). While we have not done an exhaustive test to ask whether any of the other centromeres was replicated in *rad53* cells in HU, we note that we have never been able to detect any shift toward hybrid DNA for the genome as a whole or even for efficient, early firing origins such as *ARS305* and *ARS306* (data not shown). We conclude that a very small percentage of *rad53* cells are capable of replicating even a single centromere whereas, under the same conditions, *mec1 sml1* cells can potentially duplicate at least three centromeres (*CEN2*, *-3*, and *-12*).

Two concurrent studies showed that chromosomes remained monopolarly tethered to one of the spindle pole bodies (SPBs) during premature spindle extension in HU-treated checkpoint mutants (KRISHNAN *et al.* 2004; BACHANT *et al.* 2005). It was proposed that, for *rad53* cells, it was due to the lack of centromere replication in HU that the chromosomes fail to biorient and the cells undergo precocious spindle extension (BACHANT *et al.* 2005). This hypothesis is consistent with our finding that *rad53* cells failed to replicate centromeres during exposure to HU.

Replication resumption after HU exposure: To ask whether the difference in the extent of replication by *rad53* and *mec1 sml1* cells in the presence of HU has an impact on how cells recover once HU is removed, we measured the progress of replication after removal of HU. Density transfers (Figure 3A) were identical to those described earlier with the exception that after cells were exposed to HU for 1 hr, they were filtered and allowed to recover in fresh light medium without HU for up to 2 hr. The extent of genomic DNA replication was measured by hybridization with total genomic DNA (Figure 3B). We found that *rad53* cells were able to recover from HU and replicate the bulk of the genome (Figure 3B), including the centromeres (Figure 3C; Figure S3), by 120 min. In contrast, *mec1 sml1* cells accumulated far less HL DNA (<50%) during the same recovery period (Figure 3, B and C). These observations suggest that *mec1 sml1* cells were less capable of resuming synthesis after exposure to HU than *rad53* cells.

We hybridized HH and HL DNA from these recovery samples to microarrays to investigate which parts of the genome were able to resume replication. By comparing samples that had recovered for 45 min after a 1-hr HU exposure to a sample of WT control cells that were also given a 45-min recovery period following a 2-hr exposure to HU, we observed that the temporal order of replication in the *rad53* and *mec1 sml1* mutants was altered: WT cells simply resumed a normal pattern of chromosome replication; however, for both *mec1 sml1* and *rad53* cells accumulation of HL DNA in normally early replicating regions was delayed relative to later replicating regions, resulting in rather flat replication profiles (Figure 3C, Figure S3). These results are consistent with the notion that in the mutants, replication forks become "damaged" and are less likely to resume replication after HU exposure. Therefore, the cells would need to rely on initiation of new forks from any unused late/dormant origins to complete genome replication.

High level of chromosome breakage after HU exposure in *mec1 sml1* but not *rad53* cells: As budding

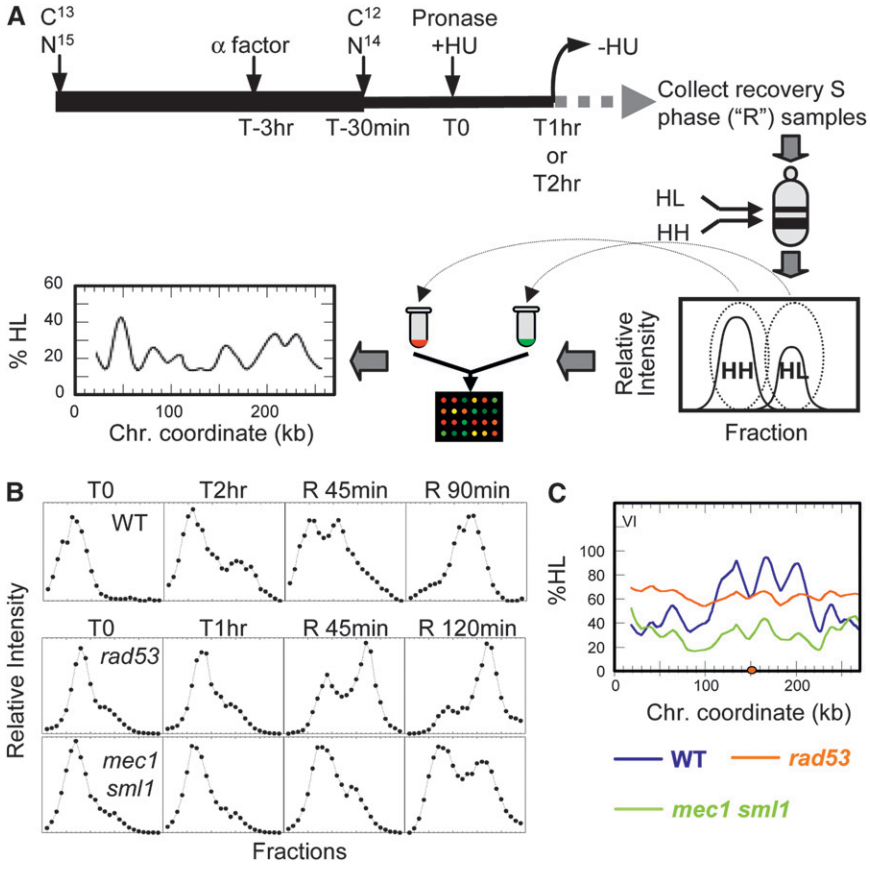

FIGURE 3.—Resumption of DNA synthesis after transient HU exposure in *mec1 sml1* (WFY73) *vs. rad53* (WFY34) cells. HM14-3a cells were used as a WT control. (A) Experimental scheme for density transfer coupled with microarray analysis. Density transfer and DNA isolation procedures were identical to those described in Figure 2 except that after cells had been transferred from dense to light medium and exposed to HU for 1 hr (for *rad53* and *mec1 sml1* cells) or for 2 hr (for WT cells), HU was removed from the culture by filtration and the cells were resuspended in fresh medium containing light isotopes and allowed to recover. Samples were removed at intervals during this "recovery" S phase (labeled as "R" samples). The "HH" and "HL" pools were differentially labeled with Cy-conjugated dUTP (Amersham) and cohybridized to a microarray. The smoothed %HL values were plotted against chromosome coordinates to generate replication profiles. (B) Slot blot results of CsCl gradients of WT (top), *rad53* (middle), and *mec1 sml1* (bottom) samples using genomic DNA as probe. (C) Replication dynamics of *rad53* R45 sample (orange) and *mec1 sml1* R45 sample (green), along with a WT control sample recovering for 45 min from a 2-hr HU exposure (blue). The orange dot indicates the centromere. For whole genome plots, see Figure S3.

yeast cells assemble intranuclear mitotic spindles during S phase, it has been suggested that early replication of centromeres might be crucial for ensuring bipolar attachment of the chromosomes during S phase and thus their proper segregation later in mitosis (TANAKA *et al.* 2005). If *mec1 sml1* but not *rad53* cells were able to duplicate at least some of their centromeres during HU exposure, then *mec1 sml1* cells would have a much higher probability of at least a few chromosomes achieving bipolar attachment during HU treatment and thereby reducing overall spindle extension. However, because *mec1 sml1* cells have difficulty in completing replication after HU is removed, we would predict that they might be prone to chromosome breakage during recovery from HU.

We used CHEF gel electrophoresis to examine the chromosomes in cells following transient exposure to HU. Cells that had been exposed to HU for 1 hr were washed and resuspended in fresh medium without HU and samples were collected every hour for up to 3 hr. Chromosome breakage was assayed by Southern blotting using probes located near the ends of specific chromosomes. For all three strains (WT, *rad53*, and *mec1 sml1*) chromosomes remained mostly intact for up to 3 hr in HU, with *mec1 sml1* cells experiencing a slightly elevated level of chromosome IX breakage (Figure 4A). However, upon the removal of HU at 1 hr, *mec1 sml1* cells showed substantial chromosome breakage, while *rad53* cells were comparable to WT cells (Figure 4A). Similar results were obtained with a chromosome V probe (data not shown).

If the chromosome breakage in *mec1 sml1* cells resulted from tension exerted by the spindle on the partially replicated chromosomes, we would expect that blocking spindle extension via nocodazole treatment would prevent or reduce chromosome breakage during recovery from HU. To test this hypothesis, we released *mec1 sml1* cells from the G1 block into medium containing HU ("HU") or HU and nocodazole ("HU+Noc") and, after a 1-hr exposure, allowed them to recover in just fresh medium ("−Noc") or in the continued presence of nocodazole ("+Noc") (Figure 4B). As expected, for the samples recovering in the absence of nocodazole ("−Noc") most of the genomic DNA was reduced to fragments of a median size of ~200 kb (Figure 4B). In contrast, fragmentation was greatly reduced in cells that recovered in the presence of nocodazole ("+Noc") leaving chromosomes mostly intact. This result supports our hypothesis that the incompletely replicated chromosomes in *mec1 sml1* cells break directly or indirectly as a consequence of tension exerted by the spindle. The residual breakage occurring in the presence of nocodazole could be attributed to either incomplete blockage of spindle extension by nocodazole or spontaneous breakage that occurred independently of tension.

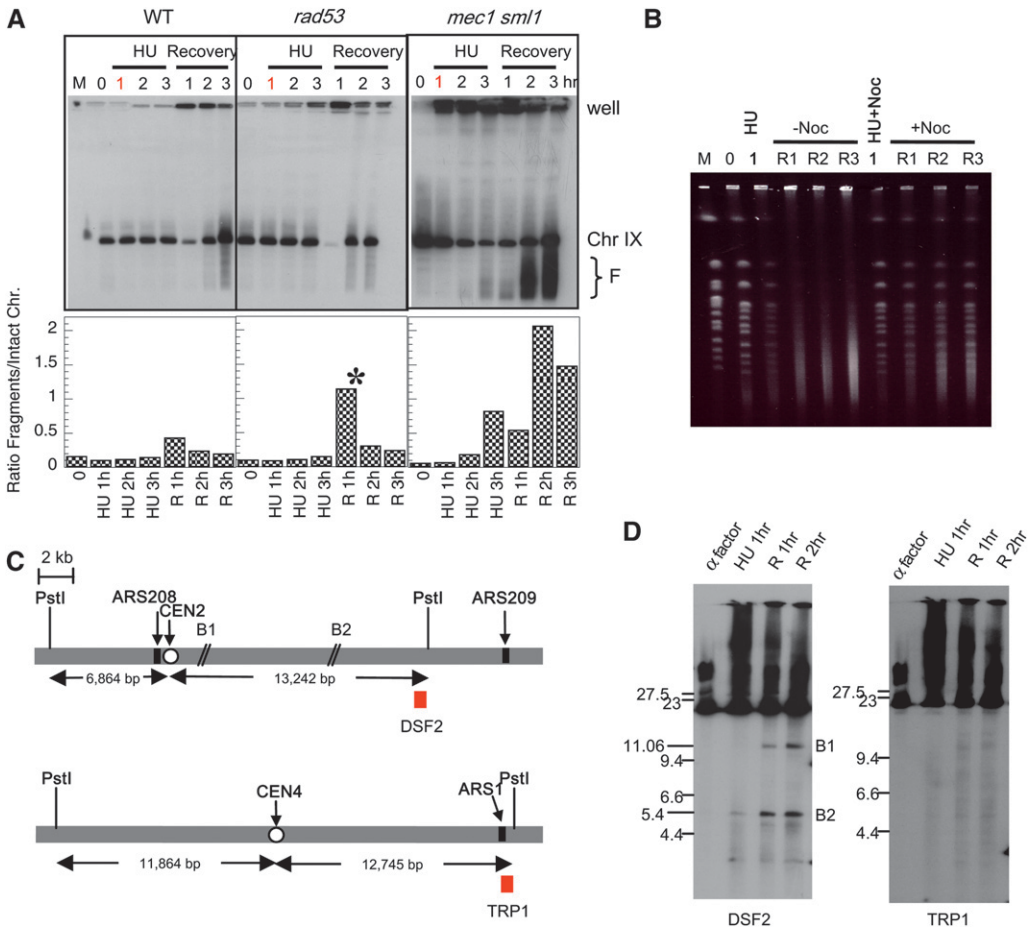

FIGURE 4.—*mec1 sml1* but not *rad53* cells show chromosome breakage during recovery from transient (1 hr) exposure to HU in S phase. (A) Top: CHEF gel and Southern blot (probed with a telomeric-proximal Chr IX probe) of WT (HM14-3a), *mec1 sml1* (WFY73), and *rad53* (WFY34) cells exposed to HU continuously for up to 3 hr (HU: 1, 2, and 3 hr) or, after 1-hr exposure to HU, allowed to recover for another 3 hr (recovery: 1, 2, and 3 hr). M, yeast chromosome markers; 0, α factor-arrested cells. The positions of sample wells, intact chromosomes, and fragmentation products (F) are indicated. Bottom: Chromosome breakage expressed as relative ratios of fragmented to intact chromosomes, quantified from relative pixel counts from the Southern blots on a Packard InstantImager Electronic Autoradiography system. Note that the ratio for the R1h sample of *rad53* (marked by an asterisk) is unreliable because most of the chromosomes remained trapped in the well. (B) Comparative analyses of chromosome breakage in *mec1 sml1* cells exposed to HU only (HU) or HU and nocodazole (HU+Noc) for 1 hr and released into media without nocodazole (−Noc, R1-3; *i.e.*, recovery: 1, 2, and 3 hr) or with nocodazole (+Noc, R1-3; *i.e.*, recovery: 1, 2, and 3 hr). CHEF gel electrophoresis followed by ethidium bromide staining is shown. (C and D) Chromosome breakage detected near *CEN2* but not *CEN4*. (C) The structures of the *Pst*I fragments containing *CEN2* and *CEN4*, respectively. (D) Chromosomal DNA from *mec1 sml1* cells recovering from 1-hr exposure to HU was embedded in agarose and in-gel digested with *Pst*I before electrophoretic separation. Southern blotting was performed with probes indicated in C as red blocks. The two breakage sites (B1 and B2) near *CEN2* are indicated.

Chromosome breakage near the centromere in *mec1* cells: If spindle tension on the bioriented centromeres of partially duplicated chromosomes is responsible for some of the breaks in the *mec1 sml1* cells recovering from HU treatment, then breaks should be detected near centromeres such as *CEN2* but not *CEN4* because *CEN2* has a higher probability of being duplicated during HU treatment than *CEN4*. We employed an indirect end-labeling method to ask whether *in vivo* breakage occurs near *CEN2* and *CEN4*. *mec1 sml1* cells at different stages of HU treatment and recovery was embedded in agarose plugs and genomic DNA was digested in-gel with *Pst*I, which generates 20-kb and 24.6-kb fragments containing *CEN2* and *CEN4*, respectively (Figure 4C). Hybridizing the Southern blot with probes located near the end of each fragment (*DSF2* for Chr II and *TRP1* for Chr IV, Figure 4C) allowed us to detect and map the potential sites of chromosome breakage on each fragment.

We detected two breakage sites in the pericentric region of *CEN2*, labeled B1 and B2, located ~2 kb and 10 kb to the right of *CEN2*, respectively (Figure 4, C and D). Breakage at B1 is observed only during recovery; breakage at B2 is detected during HU treatment but increases in frequency during recovery (Figure 4D). The relative percentages of breakage at these sites at 2 hr during recovery are 3.8 and 4.9% for B1 and B2, respectively. These values are consistent with the notion that chromosome breakage occurs at a low rate at any given locus but collectively contribute to the overall level of chromosome breaks. Neither breakage is detected in α-factor arrested cells, suggesting that replication is required to generate both breaks (Figure 4D). In contrast, no significant sites of breakage near *CEN4* were observed using a *TRP1* probe on the right end of the *Pst*I fragment on Chr IV (Figure 4D). These observations are consistent with our hypothesis that incompletely replicated chromosomes in HU-treated *mec1 sml1* cells are subject to

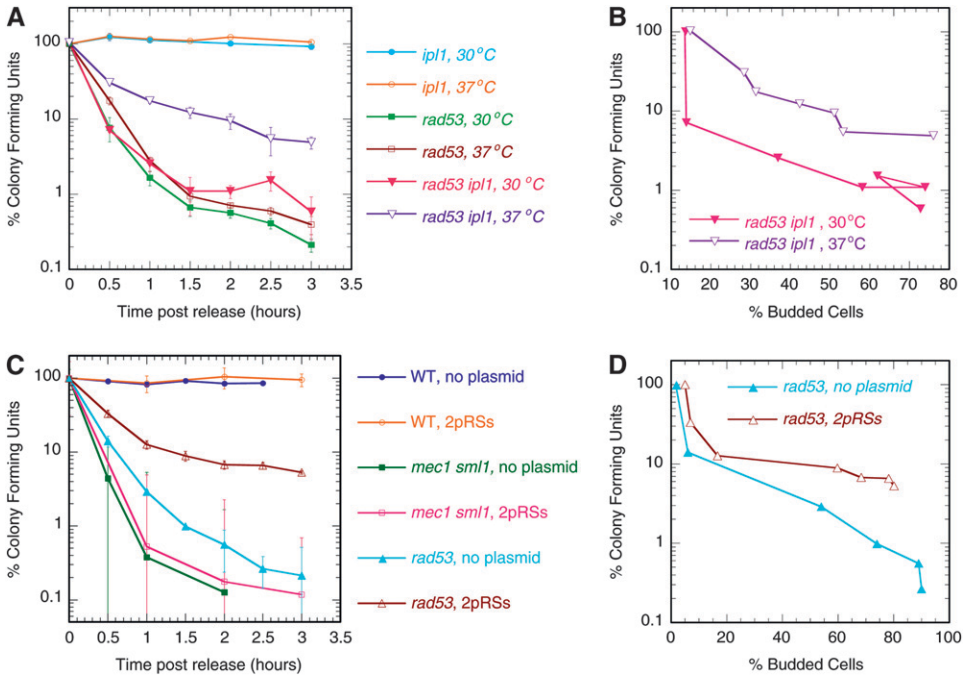

FIGURE 5.—Lethality in *rad53* cells in HU can be partially rescued by inactivating the Ipl1 kinase (A and B) or by the introduction of CEN-ARS plasmids (C and D). The percentage of colony forming units was calculated for each sample by normalizing to the control T0 sample. Error bars represent standard deviations. (A) Effect of the *ipl1-321* temperature sensitive mutation on viability of *rad53* cells released into HU at 30° or 37°. *ipl1* (SBY630), *rad53* (WFY88), and *ipl1 rad53* (WFY80) cells are shown. (B) The cell viability of *ipl1 rad53* cells at 30° and 37° described in A was plotted against percentage of budded cells at the respective temperature. (C) Viability of cells with or without CEN-ARS plasmids (pRS315 and pRS316) in HU. (D) Viability of *rad53* cells transformed with the two plasmids or no plasmid described in C was plotted against the percentage of budded cells for comparison of cell viability at equivalent cell cycle stages.

breakage, and that at least some of this breakage occurs as a direct consequence of bipolar spindle force.

Partial improvement of *rad53* cell viability by eliminating reorientation of kinetochore-to-SPB connections: If *rad53* cells can resume replication after HU removal rapidly enough to escape chromosome fragmentation, why do they die after exposure to HU? We propose that at least one type of lethal event in *rad53* cells in HU is the precocious segregation of chromosomes with an unreplicated centromere that can only experience monopolar attachments. Furthermore, if the spindle assembly checkpoint (SAC) is active during the HU-challenged S phase, then attachments to the old spindle will be repeatedly broken as the error correction mechanisms attempt to biorient chromosomes by distributing attachments between the two spindle poles. With randomly oriented, unreplicated centromeres, the genome would undergo a reductional segregation toward the two spindle poles.

This proposed scenario is reminiscent of the phenotype of a *cdc6* mutant that is defective in the initiation of DNA synthesis—*cdc6* cells undergo reductional mitosis to randomly segregate their intact unreplicated chromosomes (HARTWELL 1976; BUENO and RUSSELL 1992; LIANG *et al.* 1995; PIATTI *et al.* 1995). However, in a *cdc6 ipl1* double mutant (*IPL1* encodes the yeast homolog of the mammalian Aurora B kinase) (CHAN and BOTSTEIN 1993; BIGGINS *et al.* 1999), the chromosomes predominantly remain attached to the old spindle pole (TANAKA *et al.* 2002). Consequently, all the chromosomes segregate to the daughter cell (TANAKA *et al.* 2002). Therefore, we hypothesized that inactivating the Ipl1 kinase to avert the reductional mitosis might improve *rad53* cell viability in HU by increasing the chance that one of the cells would inherit the entire genome and proceed with replication once HU is removed.

A *rad53 ipl1* culture was split upon release from α-factor arrest, with one half incubated at 30° (the permissive temperature for the *ipl1-321* mutation), and the other half at 37° (the nonpermissive temperature). Cells incubated at 37° showed significantly higher levels of viability than did the cells incubated at 30° (Figure 5A). This observation held true even after we accounted for the difference in cell cycle entry kinetics at the two temperatures (Figure 5B). The viability of either single mutant was unaffected by temperature (Figure 5A). These results support our predictions that (1) the inactivation of the Ipl1 kinase would allow at least some of the *rad53* cells to inherit a full genome in the presence of HU, and (2) during recovery from HU, *rad53* cells would be able to finish replicating the bulk of their chromosomes and retain viability. Among the *rad53 ipl1* cells that had survived HU exposure, we would expect to find some cells with greater than one genome equivalent of DNA content. We screened 14 colonies of *rad53 ipl1* HU survivors by flow cytometry. Most of these colonies gave rise to cultures that were heterogeneous in DNA content, ranging from one to two genome equivalents, indicative of aneuploidy (Figure S4).

Because the *ipl1* mutation is defective in the tension-sensing branch of the SAC, it is formally possible that it

is the inactivation of the SAC rather than the elimination of the kinetochore-to-pole reorientation that rescues *rad53* lethality in HU. If this postulate were true, then one would expect that the inactivation of the SAC via a mutation in the *MAD2* gene would also rescue *rad53* lethality in HU. We found that the double mutant *rad53 mad2*Δ did not have elevated viability in HU compared to the *rad53* single mutant (Figure S5). Therefore, we conclude that *ipl1* mutation rescues *rad53* HU sensitivity by forcing all chromosomes to cosegregate with the same pole, thereby preventing reductional segregation of the genome.

Partial restoration of *rad53* cell viability in HU by CEN-ARS plasmids: We have estimated from the *mec1 sml1* cells that a minimum of three duplicated centromeres is sufficient to block precocious spindle extension and random segregation of the genome. Previously, it was demonstrated that the introduction of multiple CEN-ARS plasmids in which a centromere was placed immediately adjacent to an ARS to increase the number of replicated centromeres was able to reduce the level of spindle extension in *rad53* cells in HU (Bachant *et al.* 2005). We wanted to ask whether reinforcing bipolar attachment would actually ameliorate the loss of viability in *rad53* cells in HU. We tested both *mec1 sml1* and *rad53* cells bearing two CEN-ARS plasmids (pRS314 and pRS316) for their ability to form colonies after HU treatment.

Cells grown under selection for the plasmid markers were released from a G1 arrest into selective medium containing HU. Samples were collected during S phase and plated on nonselective medium lacking HU. At the time of transfer the culture was quite heterogeneous with only 30% of the population containing both plasmids. Therefore we chose *not* to select for the presence of the plasmids after cells were plated because we wanted to examine specifically whether the subset of cells that actually contained plasmids were able to improve cell viability during HU exposure, not whether the ensuing plasmid replication and segregation were successful. After 3 days of incubation, colonies were counted to calculate the relative viability of cells over time in HU.

The culture of *rad53* cells transformed with the two CEN-ARS plasmids had improved viability (~10% at 3 hr in HU) when compared to the control cells without the plasmids (<1% at 3 hr in HU) (Figure 5C). To ensure that the improved survival was not simply due to slowed S phase entry of the transformed cells, we also compared cell viability at times when the two cell cultures had reached similar levels of budding or cell cycle entry. To make this comparison, we plotted the cell viability as a function of the budding indices (Figure 5D). This plot confirms that the viability of cells that contained plasmids was higher than that of control cells at the same cell cycle stage. Moreover, rescue was specific to the *rad53* mutant, as we did not observe any increase in viability of *mec1 sml1* cells with the plasmids (Figure 5C). Thus, we conclude that increasing the number of centromeres in *rad53* cells that could potentially be replicated in the presence of HU, and thus become bioriented, stabilizes the mitotic spindle and prevents the precocious random segregation of chromosomes with only monopolar attachment.

***rad53* mutants are unable to biorient or separate chromosomes after HU treatment:** Our observations thus far are consistent with the hypothesis that *rad53* cells suffer from reductional chromosome segregation during HU treatment, but can substantially replicate centromeres following removal of HU. To determine if these replicated centromeres can establish bipolar connections to the spindle, we compared the ability of *rad53K227A*, *rad53-21*, and *mec1*Δ *GAP-RNR3* cells to recover chromosome biorientation following a 1-hr HU treatment; *rad53-21* is a well-characterized S phase checkpoint defective allele (Allen *et al.* 1994) and *mec1*Δ *GAP-RNR3* (where the essential function of *MEC1* is compensated by the overproduction of *RNR3* under the **g**lycer**a**ldehyde 3-phosphate dehydrogenase **p**romoter, similar to the *sml1* mutation; Desany *et al.* 1998) is phenotypically identical to *mec1-1 sml1*. A *cdc23-1* mutation was introduced to block anaphase entry and allow ample time for chromosome biorientation. The centromere on Chr IV was tagged with GFP (*CEN4*-GFP) to assay biorientation (Goshima and Yanagida 2000); bipolar attachment normally causes sister CENs to split into two distinct GFP foci. Following a 1-hr exposure to HU, we observed that WT and the *mec1*Δ *GAP-RNR3* mutant exhibited fairly similar kinetics of biorientation. Both *rad53* mutants, however, largely failed to achieve biorientation (Figure 6).

Defective biorientation in *rad53* cells would be expected to activate the SAC, leading to a Mad2-dependent delay in sister chromatid separation and progression through the metaphase-to-anaphase transition. Indeed, we found the anaphase inhibitor Pds1/securin (Yamamoto *et al.* 1996) was stabilized in *rad53* cells for up to 5 hr after a 1-hr HU exposure. This stabilization was largely alleviated in a *rad53 mad2*Δ double mutant (Figure S6, A and B). We also examined sister chromatid separation during HU recovery using *TRP1*-GFP near *CEN4*. Although our density transfer experiments revealed efficient replication of both *TRP1* and *CEN4* in *rad53* cells during HU recovery, very little sister chromatid separation was observed in *rad53* and *rad53 mad2*Δ strains, either when cells were washed out of HU into mating pheromone to restore a second G1 arrest or washed out into nocodazole (Figure S6, C and D). In contrast, *mad2*Δ control cells were proficient for *TRP1*-GFP separation under both conditions (Figure S6, C and D). Since the chromosome segregation defects in *rad53* cells appears to activate the SAC, these observations suggest a physical impediment to chromatid disjunction is associated with HU recovery defects in *rad53* cells.

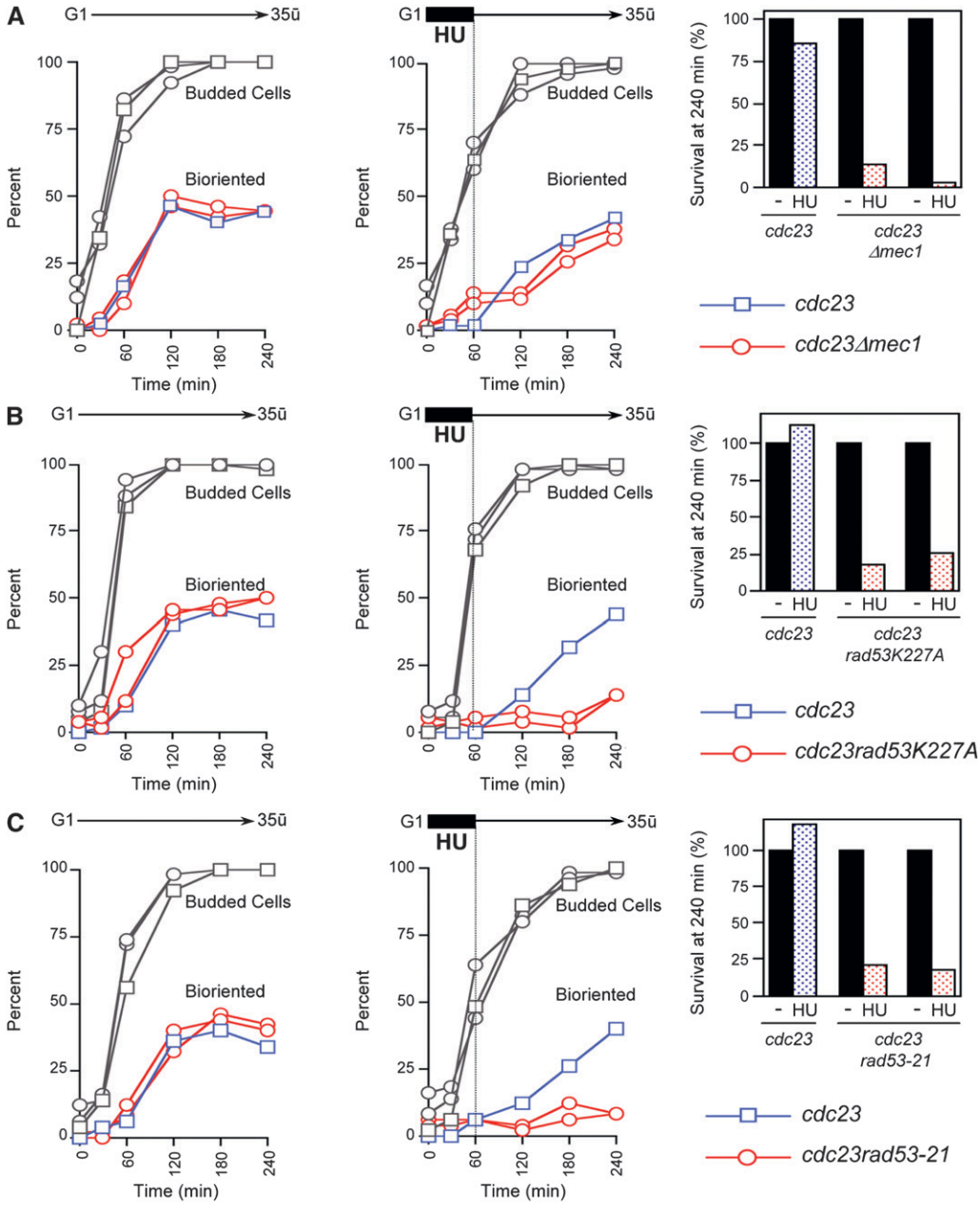

FIGURE 6.—Lack of biorientation of chromosomes in *rad53K227A* cells after removal of HU. (A) *cdc23* (JBY686) and *cdc23 mec1Δ GAP-RNR3* (JBY1720; two experiments) cells carrying *CEN4-GFP* were released from α-factor arrest into S phase in YPD media at 35° in the presence or absence of 200 mM HU for 1 hr, followed by recovery in fresh media lacking HU at 35°. At the indicated times, samples were evaluated for the percentage of cells with two separated *CEN4-GFP* foci, indicative of successful biorientation at the *cdc23* block. At the 240-min end point, cell viability was measured as the percentage of colony forming units of both HU-treated and -untreated cells; viability in the HU-untreated culture was normalized to 100%. (B) *cdc23* (JBY1726) and *cdc23 rad53K227A* (JBY1728, JBY1729; two independent isolates) cells and (C) *cdc23* (JBY1732) and *cdc23 rad53-21* (JBY1735, JBY1736; two independent isolates) cells with *CEN4-GFP* were processed and scored as described in A.

DISCUSSION

Why replication-checkpoint-deficient yeast cells die when challenged with a replication impediment is a long-standing question. Do cells die because they cannot complete some aspect of genome replication after the impediment is removed, or is it because, in the absence of the checkpoint, they have executed some critical cell cycle events out of order? Characterizing replication and segregation phenotypes of mutants in two checkpoint kinases, we have been able to distinguish how failure of each of these two processes contributes to distinct types of genome instability (Figure 7).

We found that when *rad53* cells encounter HU in S phase they are unable to duplicate their centromeres and therefore do not achieve the bipolar attachment that normally occurs early in S phase to generate tension within the spindle. As a consequence of premature spindle elongation, unreplicated chromosomes become randomly partitioned to the two spindle poles. Though *rad53* cells are capable of nearly completing genomic DNA replication after the removal of HU, we propose that by the time that replication restarts, the window of opportunity to establish bioriented chromosomes has passed and/or that *rad53* cells suffer from specific defects that preclude chromosome biorientation (such as structural defects of the centromeres and/or kinetochores) or sister chromatid disjunction during recovery from HU. Thus, *rad53* cells are destined for

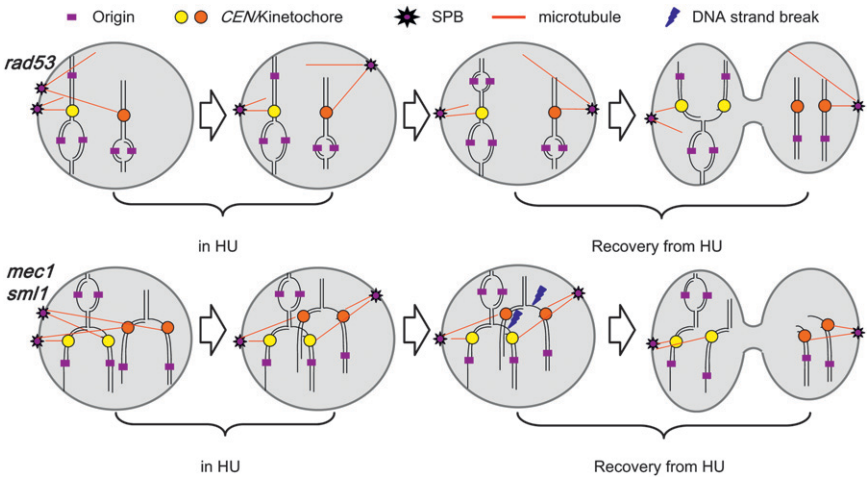

Figure 7.—A model for the differential chromosomal behaviors in *rad53* and *mec1* cells upon exposure to HU. Two representative chromosomes are depicted. The centromeres and their associated kinetochores, origins of replication, spindle pole bodies, and spindles are labeled as indicated in the legend. In *rad53* cells, upon HU exposure, replication forks initiated from nearby origins do not reach the centromeres, failing to duplicate them. Meanwhile, SPB duplicates and chromosomes are randomly attached to one of the two SPBs in a monopolar fashion, followed by SPBs separation in the absence of tension on the spindle. After HU is removed, despite substantial replication through resumption of replication forks (on the chromosome with orange centromere) or new initiation events (on the chromosome with yellow centromere), the genome is randomly segregated to opposite poles. In *mec1 sml1* cells, replication forks are able to reach and duplicate some centromeres and establish bipolar attachment of the chromosomes. But the failure to finish replicating the chromosomes causes them to break under tension on the spindle after HU is removed.

random chromosome segregation by both precocious spindle extension during HU treatment and lethal defects in chromosome attachment/separation after HU removal. In contrast, *mec1 sml1* cells are largely proficient for bipolar attachment but experience lethal chromosome breaks due to nondisjunction of incompletely replicated chromosomes. Although the force exerted by a spindle microtubule (Nicklas 1983; Bloom 2008) is thought to be insufficient to make a dsDNA break (Bensimon *et al.* 1995), the presence of ssDNA brings spindle force-induced breakage into the realm of possibility. Alternatively, spindle force may induce chromatin unraveling, making regions more accessible to nucleases—an idea consistent with our observation of discrete breakage sites (Figure 4D; see File S1 for a fuller discussion).

While we refer to these differences in replication and cell cycle execution as resulting from the loss of Rad53 or Mec1 checkpoint function, we do not mean to imply that we have necessarily detected distinct functions for Rad53 and Mec1 kinases in the DNA replication checkpoint pathway. It may be the case that Rad53 and Mec1 kinases do have distinct phosphorylation targets, and that the two mutations reflect these differences. However, there are at least two other explanations for the phenotypic differences that we have observed in the two mutants. (1) The different point mutations in the *rad53K227A* and *mec1-1 sml1* alleles may retain different residual levels of checkpoint activation and the specific phenotypes may reflect this difference. (2) The *mec1 sml1* strain may have higher level of dNTPs than *rad53* due to the *sml1* mutation. However, we were informed that by chromatin immunoprecipitation of bromodeoxyuridine-labeled DNA coupled with microarray analysis, it was observed that *mec1* mutants (*mec1-1* and *mec1-100*) consistently showed longer tracks or more extensive fork progression than a *rad53* mutant (*rad53-11*) in the presence of HU (L. Crabbe, P. Pasero and A. Lengronne, personal communication). Because neither the *mec1-100* nor the *rad53-11* allele requires the *sml1* mutation for survival, this observation suggests that the difference between *mec1 sml1* and *rad53* mutants may not be simply attributed to different levels of dNTPs in the cell. Regardless of which explanation is correct, the specific mutations we have used have allowed us to identify an important step in the chromosome duplication cycle that is regulated by the DNA replication checkpoint. Interestingly, another checkpoint mutant *mrc1*, which similarly exhibits precocious spindle elongation upon HU treatment, is able to maintain substantial viability (Alcasabas *et al.* 2001). However, because a detailed study of replication dynamics and chromosome segregation of *mrc1* cells under replication stress has not been performed, it is possible that *mrc1* cells can replicate some centromeres in HU as *mec1 sml1* cells do and recover replication as *rad53* cells do, thus averting both precocious chromosome segregation and chromosome breakage. Our study underscores the importance for yeast cells to execute linked steps of the cell cycle in their correct order and specifically the importance of replicating centromeres early in S phase to ensure proper spindle assembly and chromosome segregation.

A corollary of the hypothesis stated above is that restraining the spindle from extension via nocodazole treatment should ameliorate the loss of viability in *rad53* cells in HU. The addition of nocodazole *following* transient exposure to HU failed to rescue the loss of viability of *rad53* cells (Desany *et al.* 1998). We found that including nocodazole *during* the exposure to HU also did not result in improved viability (data not shown). However, we do not believe that these results should be taken to suggest that precocious spindle extension is not a principal reason for lethality in *rad53* cells after HU treatment. Rather, we speculate that

nocodazole affects not only microtubule dynamics but also the behavior of spindle poles. Indeed, we note that even treating *RAD53* cells simultaneously with HU and nocodazole during S phase for just half an hour led to a reduction of viability by ~50% (data not shown). Consistent with this finding is the observation that nocodazole not only prevents spindle pole body (SPB) separation (Yoder *et al.* 2003) but also abolishes centromere clustering near the SPBs during G1, causing them to drift away from the SPBs (Tanaka *et al.* 2002). Recent studies that followed kinetochore recapture after nocodazole treatment demonstrated that yeast mitotic chromosomes have difficulty attaching and biorienting on the spindle when the SPBs are in the unseparated (side by side) configuration, and require the functional Sgo1 protein for correction (Indjeian *et al.* 2005; Indjeian and Murray 2007). If the unduplicated kinetochores in *rad53* cells in HU were released from the SPBs to which they were first attached, subsequent duplication and recapture by both SPBs might be an inefficient and error-prone event. Therefore, nocodazole's potential ability to rescue *rad53* cell lethality in HU may be masked by its negative effect on SPB segregation and subsequent capture and biorientation of chromosomes.

We note that in the population of cells transformed with the CEN-ARS plasmids we achieved only modest increase in viability (from 3% without CEN-ARS plasmids to 12% with two CEN-ARS plasmids at 60 min in HU). While we do not know for certain how many replicated centromeres are required to restrain the spindle in WT cells, we can make estimates on the basis of our replication studies of *rad53* cells in HU. As we were unable to detect any replication of *CEN2*, which is ~500 bp from its closest origin of replication, it would leave only two centromeres as candidates, and one of these is adjacent to an ARS that is rarely used under normal circumstances (*ARS308*). If we were to assume a success rate for replication of either of these two centromeres of 20% (an estimate based on the sensitivity of our density transfer assay to detect even partial replication of fragments containing the efficient origins *ARS305* and *ARS306*), and if two replicated centromeres were sufficient to restrain the spindle to ensure viability upon recovery from HU, then we could expect a survival rate of 4%. Introducing plasmids with similarly spaced centromeres and ARSs would theoretically improve viability to ~20%. The fact that only 30% of the cells in the culture actually had both plasmids reduces the expectation of survival to be <20%. We predict that introducing origins of replication closer to additional chromosomal centromeres might demonstrate even better rescue of HU sensitivity in *rad53* cells than the CEN-ARS plasmids. Likewise, the rescue of *rad53* HU sensitivity by *ipl1* mutation was only partial presumably because many of the cells that survived are aneuploid (Figure S4) and thus suffer a growth disadvantage (Torres *et al.* 2007).

Although we have shown that *rad53K227A* cells suffer from reductional mitosis, it is difficult to ascertain how much cell death of *rad53* cells can be attributed to segregation defects as opposed to other causes. In fact, we believe that *rad53* cells also suffer substantially from replication defects during recovery from HU, despite near completion of DNA synthesis. It is noteworthy that the observation of the substantial ability of *rad53K227A* cells to replicate DNA, following transient (1 hr) exposure to HU, is somewhat at odds with a previous study where it was reported that *rad53K227A* cells are virtually incapable of DNA synthesis after exposure to HU (Lopes *et al.* 2001). We believe the difference between the two studies lies in the fact that Lopes *et al.* employed a much more extensive (3 hr) exposure of *rad53* cells to HU. We have observed that the ability of *rad53* cells to recover from HU decreased as the duration of exposure to HU increased and that the replication occurring during recovery relied even more on new initiation events in cells exposed to HU for longer period than shorter ones, suggesting that replication forks are destabilized in a time-dependent fashion in HU (data not shown). The genomic replication profiles during recovery from HU also showed that the normal replication timing pattern was somewhat reversed in both mutants, suggesting that many replication forks established during HU exposure were defective in resuming synthesis and that some portion of the observed replication during recovery may have originated from new initiation events from previously unfired origins. We are currently investigating the extent to which replication resumption in *rad53* and *mec1 sml1* cells relies on new initiations *vs.* resumption from preexisting forks and whether ssDNA gaps are filled or become sites of chromosomal breakage.

Although there are no studies that specifically examine whole-genome replication and spindle assembly in the same WT culture, we can extrapolate our results with checkpoint mutants to propose a possible role of early centromere replication during normal and HU-challenged cell cycles in WT cells. Once the cyclin-dependent kinase (CDK1) becomes active in G1 a cascade of events is initiated that sets in motion two independent pathways leading to spindle pole duplication and chromosome replication. The intra-S-phase checkpoint is responsible for making sure that the two pathways remain coordinated. We imagine that one crucial event is the early replication of at least a few centromeres. Once duplicated, the assembly of kinetochores on these centromeres and their attachment to opposite spindle poles puts a physical restraint on the spindle. In the presence of a replication-inhibiting agent such as HU, the checkpoint cascade must intervene with both chromosome replication and spindle

assembly. Engaging the checkpoint accomplishes two important replication functions: (1) stabilizing ongoing forks so that they can continue at a slow rate to incorporate nucleotides during HU treatment and can efficiently resume once HU is removed and (2) delaying activation of unfired origins so that the cell can concentrate the few available nucleotides to sites of the earliest activated replication forks—among which are those near a few centromeres.

We thank L. Breeden, B. Garvik, and S. Biggins for providing yeast strains and U. Surana for personal communications at early stages of this work. We are grateful to T. Davis, S. Biggins, B. Byers, J. Sidorova, and the Brewer/Raghuraman lab members for insightful discussions and to the anonymous reviewers for helpful suggestions. We also thank P. Pasero for personal communication of unpublished data. We extend our gratitude to the staff at the Center for Array Technologies in Seattle for microarray hybridization and scanning. This work was supported by the National Institute of General Medical Sciences (NIGMS) grant 18926 (to B.J.B. and M.K.R.). W.F. was supported by a Pathway to Independence award (1K99GM081378-01) from the National Institutes of Health.

LITERATURE CITED

Alcasabas, A. A., A. J. Osborn, J. Bachant, F. Hu, P. J. Werler *et al.*, 2001 Mrc1 transduces signals of DNA replication stress to activate Rad53. Nat. Cell. Biol. **3:** 958–965.

Allen, J. B., Z. Zhou, W. Siede, E. C. Friedberg and S. J. Elledge, 1994 The *SAD1/RAD53* protein kinase controls multiple checkpoints and DNA damage-induced transcription in yeast. Genes Dev. **8:** 2401–2415.

Bachant, J., S. R. Jessen, S. E. Kavanaugh and C. S. Fielding, 2005 The yeast S phase checkpoint enables replicating chromosomes to bi-orient and restrain spindle extension during S phase distress. J. Cell Biol. **168:** 999–1012.

Basrai, M. A., V. E. Velculescu, K. W. Kinzler and P. Hieter, 1999 *NORF5/HUG1* is a component of the *MEC1*-mediated checkpoint response to DNA damage and replication arrest in *Saccharomyces cerevisiae*. Mol. Cell. Biol. **19:** 7041–7049.

Bensimon, D., A. J. Simon, V. V. Croquette and A. Bensimon, 1995 Stretching DNA with a receding meniscus: experiments and models. Phys. Rev. Lett. **74:** 4754–4757.

Biggins, S., F. F. Severin, N. Bhalla, I. Sassoon, A. A. Hyman *et al.*, 1999 The conserved protein kinase Ipl1 regulates microtubule binding to kinetochores in budding yeast. Genes Dev. **13:** 532–544.

Bloom, K. S., 2008 Beyond the code: the mechanical properties of DNA as they relate to mitosis. Chromosoma **117:** 103–110.

Branzei, D., and M. Foiani, 2006 The Rad53 signal transduction pathway: replication fork stabilization, DNA repair, and adaptation. Exp. Cell Res. **312:** 2654–2659.

Bueno, A., and P. Russell, 1992 Dual functions of *CDC6*: a yeast protein required for DNA replication also inhibits nuclear division. EMBO J. **11:** 2167–2176.

Chan, C. S., and D. Botstein, 1993 Isolation and characterization of chromosome-gain and increase-in-ploidy mutants in yeast. Genetics **135:** 677–691.

Desany, B. A., A. A. Alcasabas, J. B. Bachant and S. J. Elledge, 1998 Recovery from DNA replicational stress is the essential function of the S-phase checkpoint pathway. Genes Dev. **12:** 2956–2970.

Feng, W., D. Collingwood, M. E. Boeck, L. A. Fox, G. M. Alvino *et al.*, 2006 Genomic mapping of single-stranded DNA in hydroxyurea-challenged yeasts identifies origins of replication. Nat. Cell Biol. **8:** 148–155.

Feng, W., M. K. Raghuraman and B. J. Brewer, 2007 Mapping yeast origins of replication via single-stranded DNA detection. Methods **41:** 151–157.

Goshima, G., and M. Yanagida, 2000 Establishing biorientation occurs with precocious separation of the sister kinetochores, but not the arms, in the early spindle of budding yeast. Cell **100:** 619–633.

Hartwell, L. H., 1976 Sequential function of gene products relative to DNA synthesis in the yeast cell cycle. J. Mol. Biol. **104:** 803–817.

Indjeian, V. B., and A. W. Murray, 2007 Budding yeast mitotic chromosomes have an intrinsic bias to biorient on the spindle. Curr. Biol. **17:** 1837–1846.

Indjeian, V. B., B. M. Stern and A. W. Murray, 2005 The centromeric protein Sgo1 is required to sense lack of tension on mitotic chromosomes. Science **307:** 130–133.

Krishnan, V., S. Nirantar, K. Crasta, A. Y. Cheng and U. Surana, 2004 DNA replication checkpoint prevents precocious chromosome segregation by regulating spindle behavior. Mol. Cell **16:** 687–700.

Liang, C., M. Weinreich and B. Stillman, 1995 ORC and Cdc6p interact and determine the frequency of initiation of DNA replication in the genome. Cell **81:** 667–676.

Lopes, M., C. Cotta-Ramusino, A. Pellicioli, G. Liberi, P. Plevani *et al.*, 2001 The DNA replication checkpoint response stabilizes stalled replication forks. Nature **412:** 557–561.

McCarroll, R. M., and W. L. Fangman, 1988 Time of replication of yeast centromeres and telomeres. Cell **54:** 505–513.

Nicklas, R. B., 1983 Measurements of the force produced by the mitotic spindle in anaphase. J. Cell Biol. **97:** 542–548.

Piatti, S., C. Lengauer and K. Nasmyth, 1995 Cdc6 is an unstable protein whose de novo synthesis in G1 is important for the onset of S phase and for preventing a 'reductional' anaphase in the budding yeast *Saccharomyces cerevisiae*. EMBO J. **14:** 3788–3799.

Raghuraman, M. K., E. A. Winzeler, D. Collingwood, S. Hunt, L. Wodicka *et al.*, 2001 Replication dynamics of the yeast genome. Science **294:** 115–121.

Sanchez, Y., B. A. Desany, W. J. Jones, Q. Liu, B. Wang *et al.*, 1996 Regulation of *RAD53* by the ATM-like kinases *MEC1* and *TEL1* in yeast cell cycle checkpoint pathways. Science **271:** 357–360.

Santocanale, C., and J. F. Diffley, 1998 A Mec1- and Rad53-dependent checkpoint controls late-firing origins of DNA replication. Nature **395:** 615–618.

Sogo, J. M., M. Lopes and M. Foiani, 2002 Fork reversal and ssDNA accumulation at stalled replication forks owing to checkpoint defects. Science **297:** 599–602.

Tanaka, K., N. Mukae, H. Dewar, M. van Breugel, E. K. James *et al.*, 2005 Molecular mechanisms of kinetochore capture by spindle microtubules. Nature **434:** 987–994.

Tanaka, T. U., N. Rachidi, C. Janke, G. Pereira, M. Galova *et al.*, 2002 Evidence that the Ipl1-Sli15 (Aurora kinase-INCENP) complex promotes chromosome bi-orientation by altering kinetochore-spindle pole connections. Cell **108:** 317–329.

Torres, E. M., T. Sokolsky, C. M. Tucker, L. Y. Chan, M. Boselli *et al.*, 2007 Effects of aneuploidy on cellular physiology and cell division in haploid yeast. Science **317:** 916–924.

Tourriere, H., and P. Pasero, 2007 Maintenance of fork integrity at damaged DNA and natural pause sites. DNA Repair (Amst) **6:** 900–913.

van Brabant, A. J., C. D. Buchanan, E. Charboneau, W. L. Fangman and B. J. Brewer, 2001 An origin-deficient yeast artificial chromosome triggers a cell cycle checkpoint. Mol. Cell **7:** 705–713.

Weinert, T. A., G. L. Kiser and L. H. Hartwell, 1994 Mitotic checkpoint genes in budding yeast and the dependence of mitosis on DNA replication and repair. Genes Dev. **8:** 652–665.

Yamamoto, A., V. Guacci and D. Koshland, 1996 Pds1p, an inhibitor of anaphase in budding yeast, plays a critical role in the APC and checkpoint pathway(s). J. Cell Biol. **133:** 99–110.

Yoder, T. J., C. G. Pearson, K. Bloom and T. N. Davis, 2003 The *Saccharomyces cerevisiae* spindle pole body is a dynamic structure. Mol. Biol. Cell **14:** 3494–3505.

Zhao, X., E. G. Muller and R. Rothstein, 1998 A suppressor of two essential checkpoint genes identifies a novel protein that negatively affects dNTP pools. Mol. Cell **2:** 329–340.

Communicating editor: N. M. Hollingsworth

GENETICS

Supporting Information
http://www.genetics.org/cgi/content/full/genetics.109.107508/DC1

Centromere Replication Timing Determines Different Forms of Genomic Instability in *Saccharomyces cerevisiae* Checkpoint Mutants During Replication Stress

Wenyi Feng, Jeff Bachant, David Collingwood, Mosur K. Raghuraman and Bonita J. Brewer

DOI: 10.1534/genetics.109.107508

A

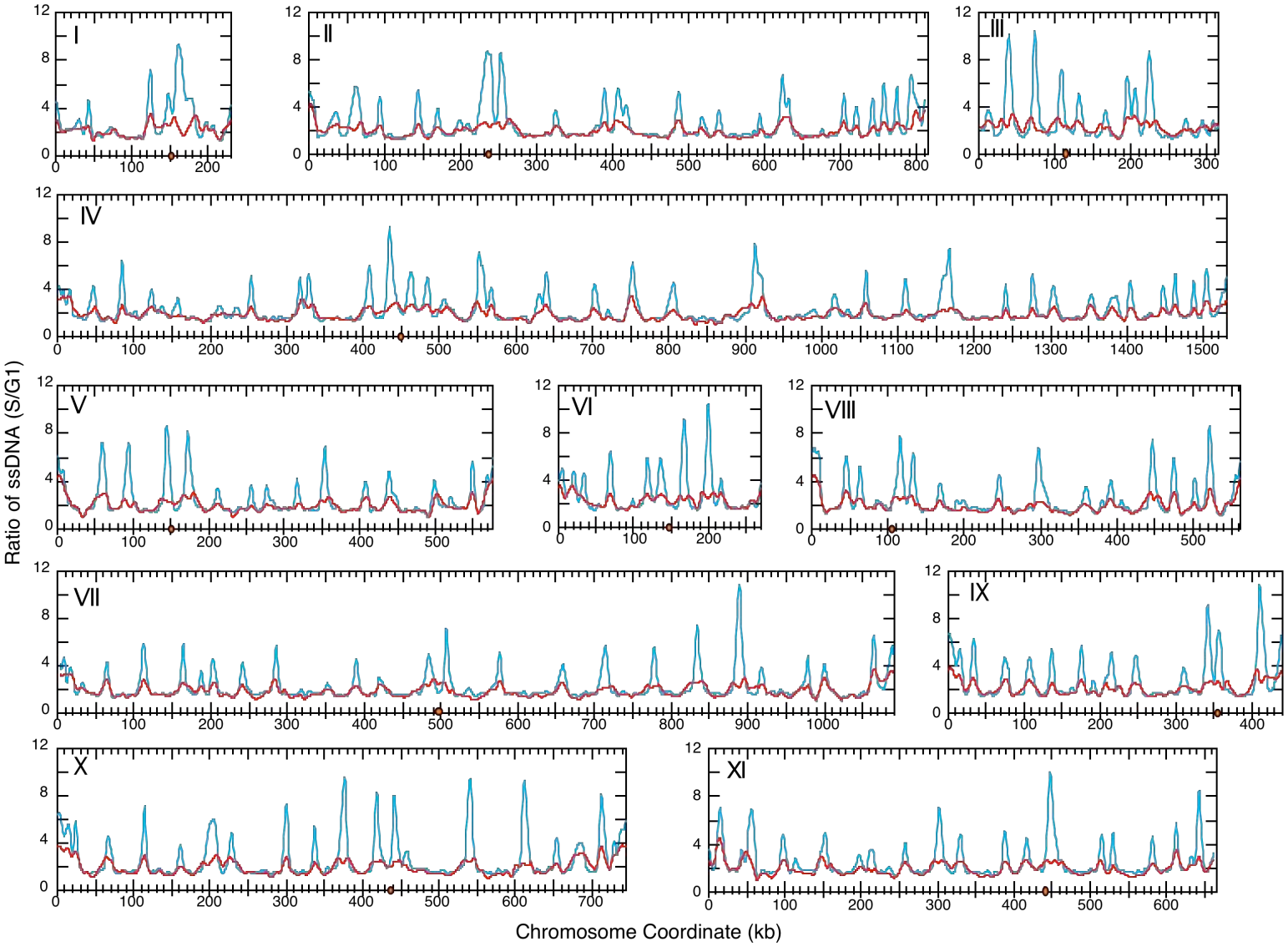
I
II
III
IV
V
VI
VIII
VII
IX
X
XI
Ratio of ssDNA (S/G1)
Chromosome Coordinate (kb)

B

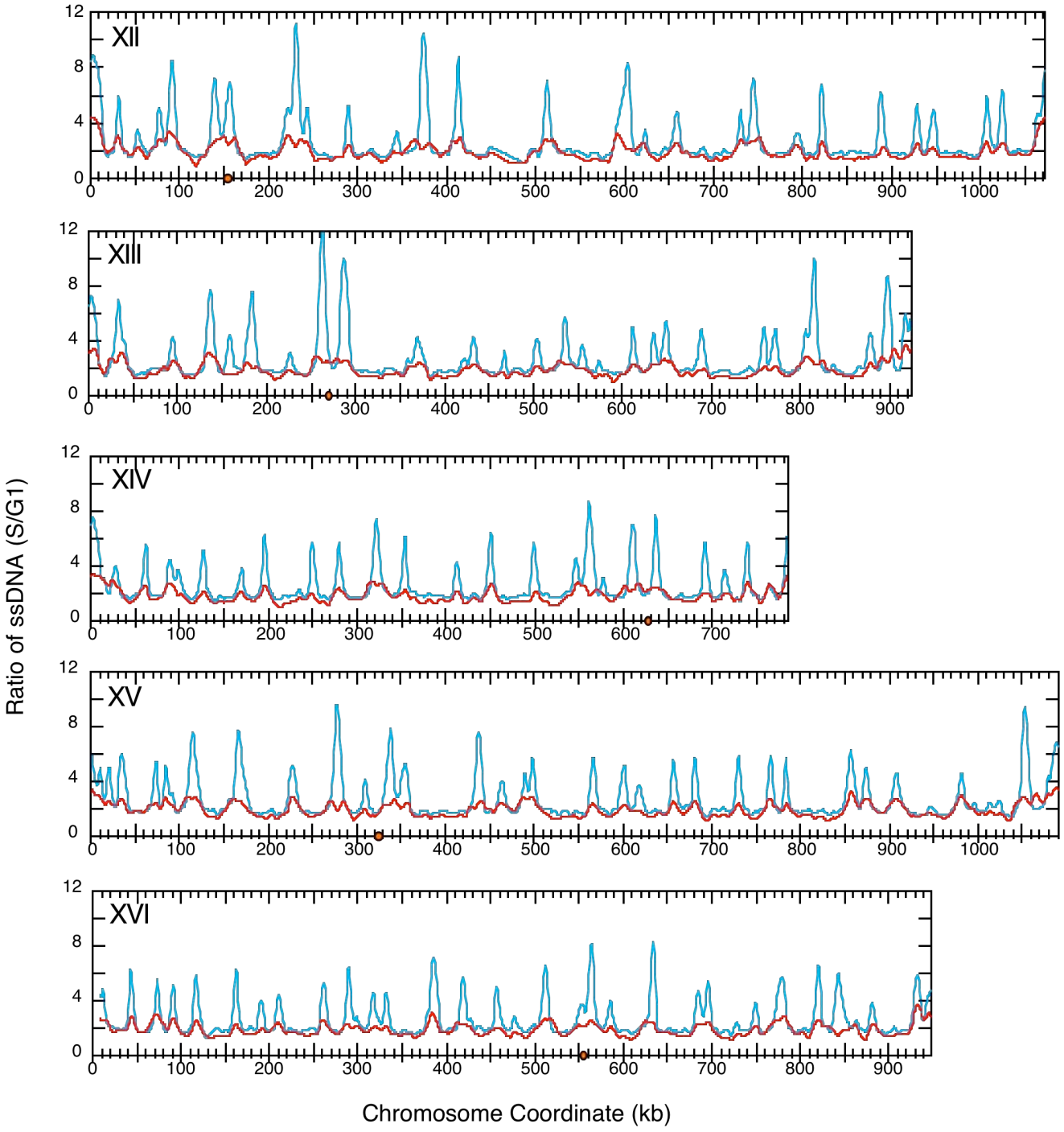

FIGURE S1.—Genomic ssDNA profiles for *rad53* and *mec1* cells after exposure to HU for 1hr. Plots show the relative ratio of ssDNA (S/G1) as a function of chromosome coordinates (kb). The ssDNA profile for *rad53* is shown in blue and that for *mec1* is shown in red. Positions of centromeres are shown as filled orange circles. The sixteen chromosomes are shown in two halves in (A) and (B).

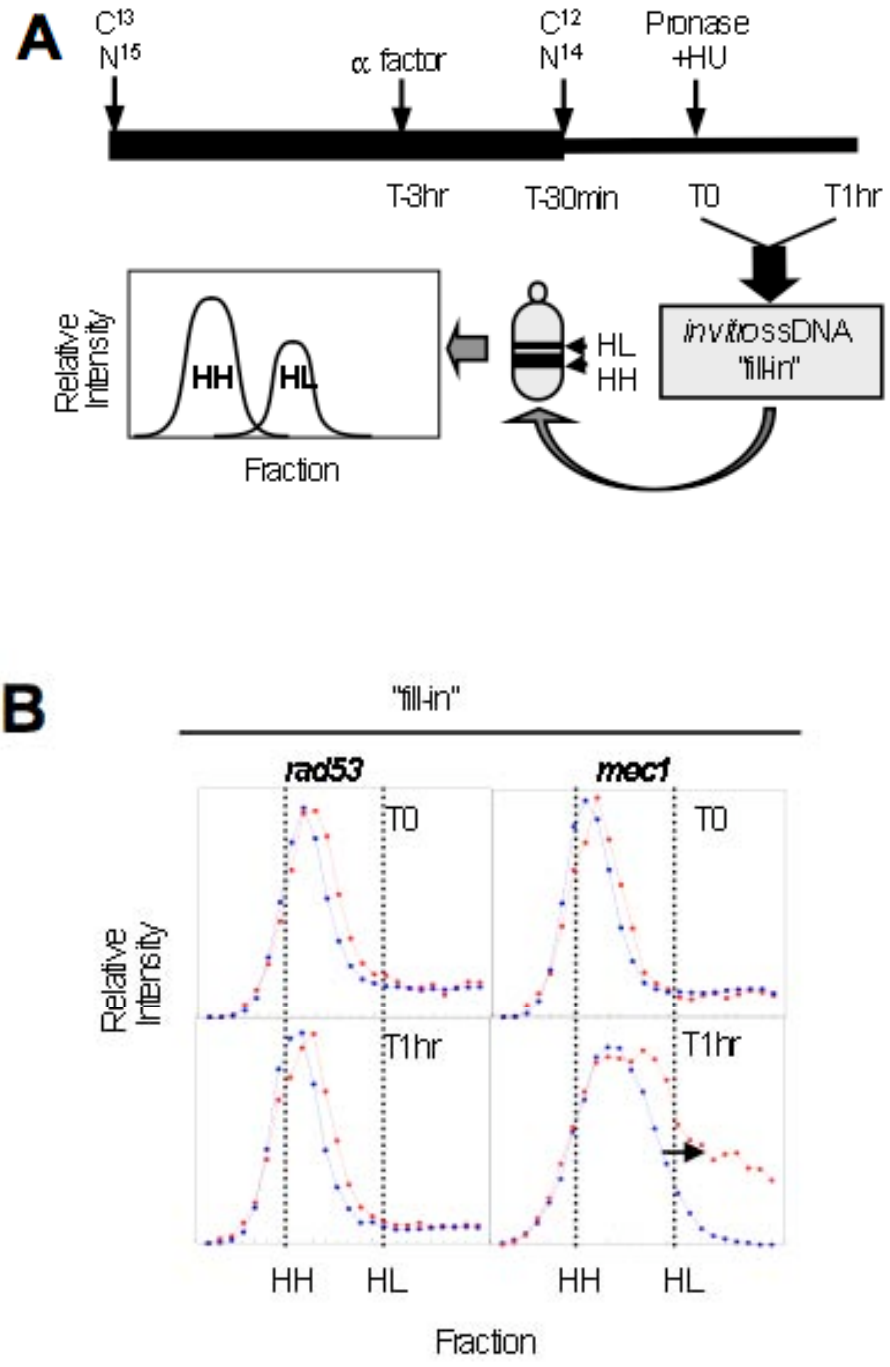

FIGURE S2.–Differences in centromere replication in *mec1* and *rad53* cells in HU after *in vitro* fill-in synthesis of ssDNA. (A) Experimental scheme for density transfer and subsequent *in vitro* fill-in synthesis in the presence of random hexameric primers, dNTPs and Klenow DNA polymerase. (B) Relative amounts of replication of the *EcoR* I fragments containing *CEN4* (blue) and *CEN2* (red) after *in vitro* fill-in synthesis of ssDNA for *rad53* and *mec1*. The spreading of the HH peak toward the position of hybrid DNA (HL) before and after *in vitro* "fill-in" synthesis is indicated by a black arrow.

A

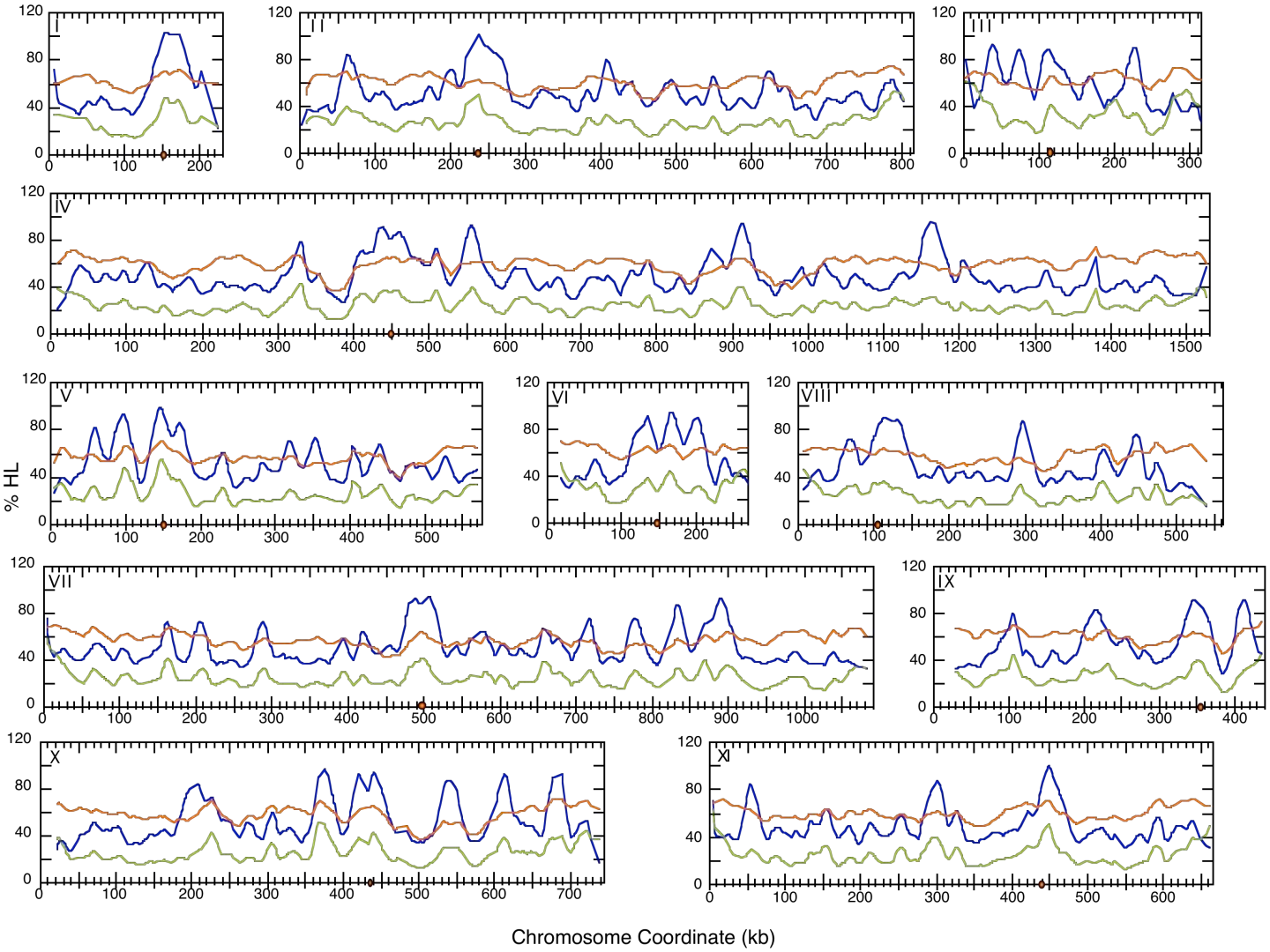

B

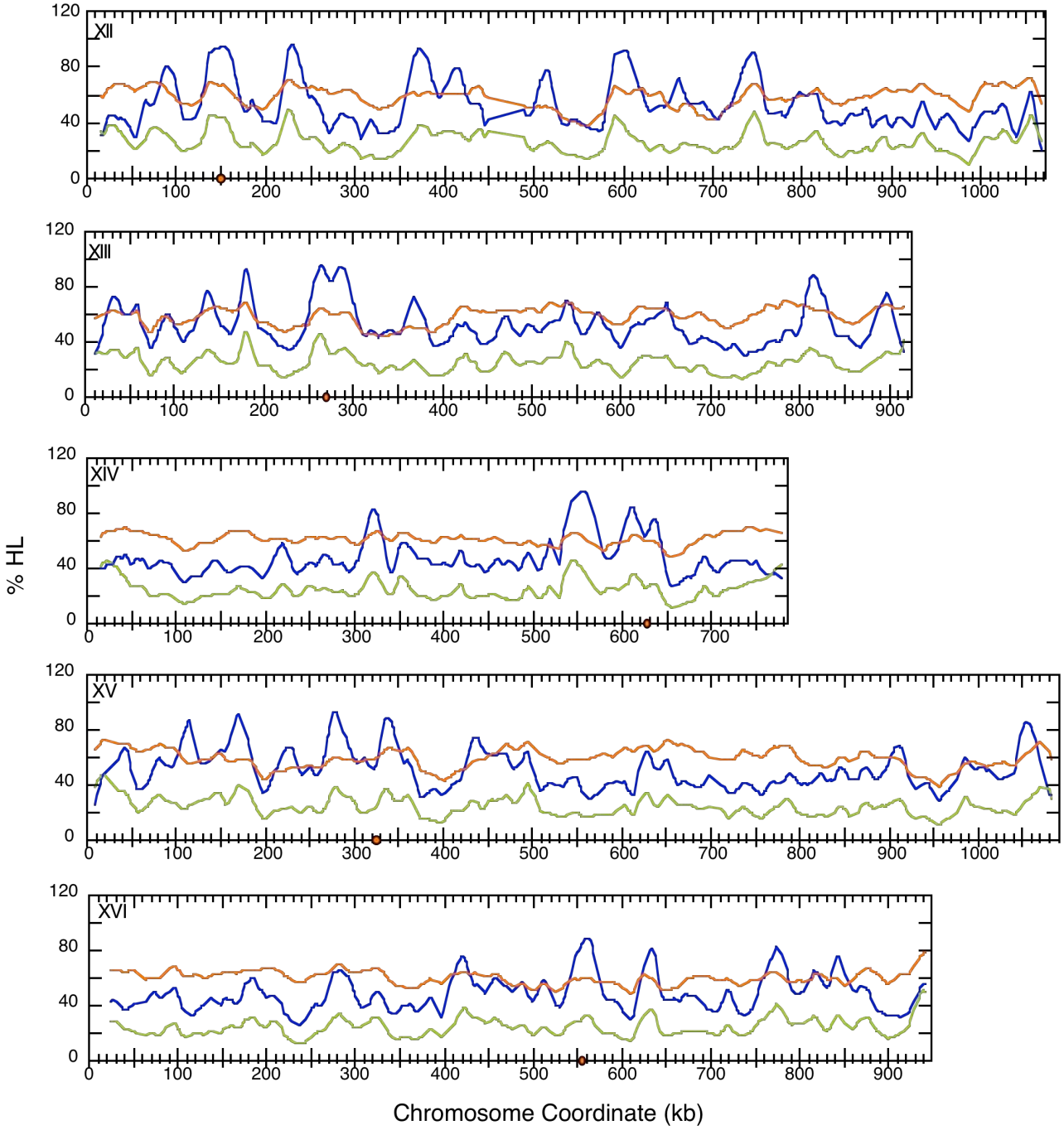

FIGURE S3.—Replication profiles of cells recovering for 45 min from a transient exposure to HU are presented. Plots show %HL as a function of chromosome coordinates (kb). The replication profile for WT cells recovering for 45 min after 2 hr HU exposure is plotted in blue. The profiles for *mec1* and *rad53* cells recovering for 45 min after 1hr HU exposure are shown in light green and orange, respectively. Centromeres are shown as orange dots. The sixteen chromosomes are shown in two halves in (A) and (B).

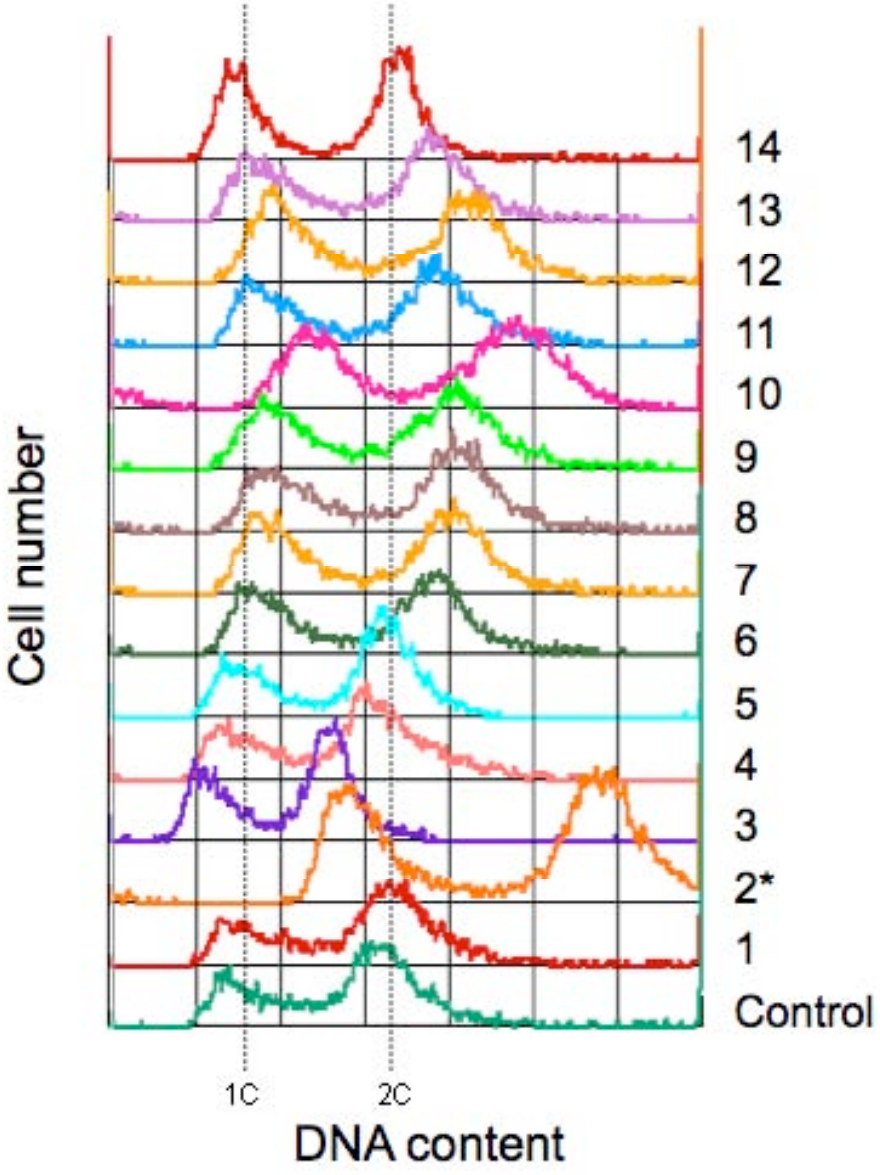

FIGURE S4.—Flow cytometry profiles of 14 independent *rad53 ipl1* cells that survived a 30 min exposure to HU. Cell number is plotted against relative fluorescence intensity. The control sample is *rad53 ipl1* cells collected during logarithmic growth. The positions of 1C and 2C DNA content are as indicated. The #2 isolate that showed approximately diploid content of DNA is indicated by an asterisk.

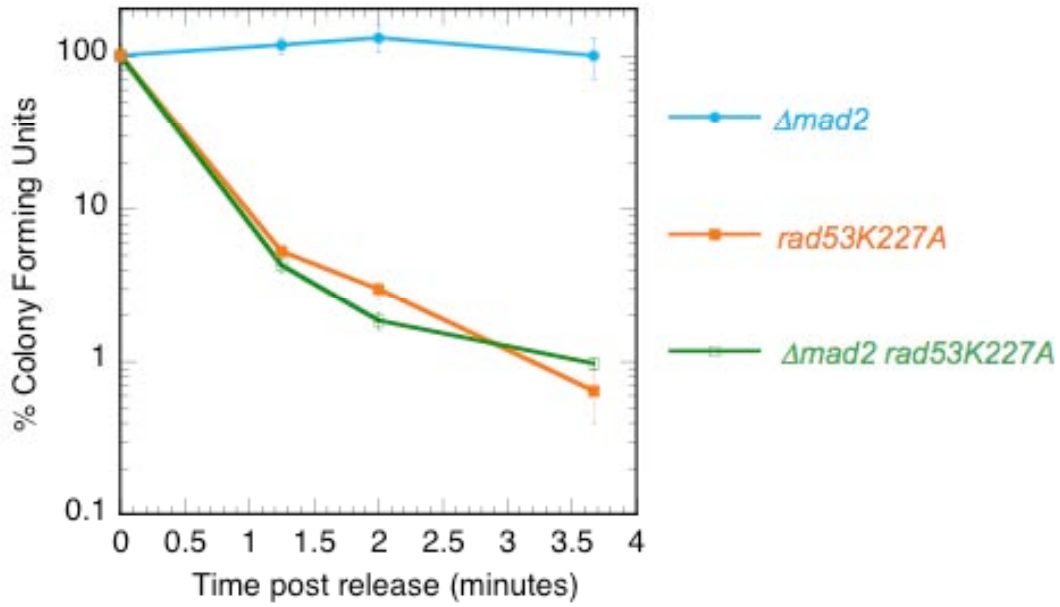

FIGURE S5.—Inactivation of the spindle activation checkpoint by *mad2Δ* mutation does not rescue the HU sensitivity of *rad53* cells. The cells were released from alpha factor arrest into media containing 200 mM HU for the indicated amount of time and the percentage of colony forming units was calculated for each sample by normalizing to the control T0 sample. Error bars represent standard deviations.

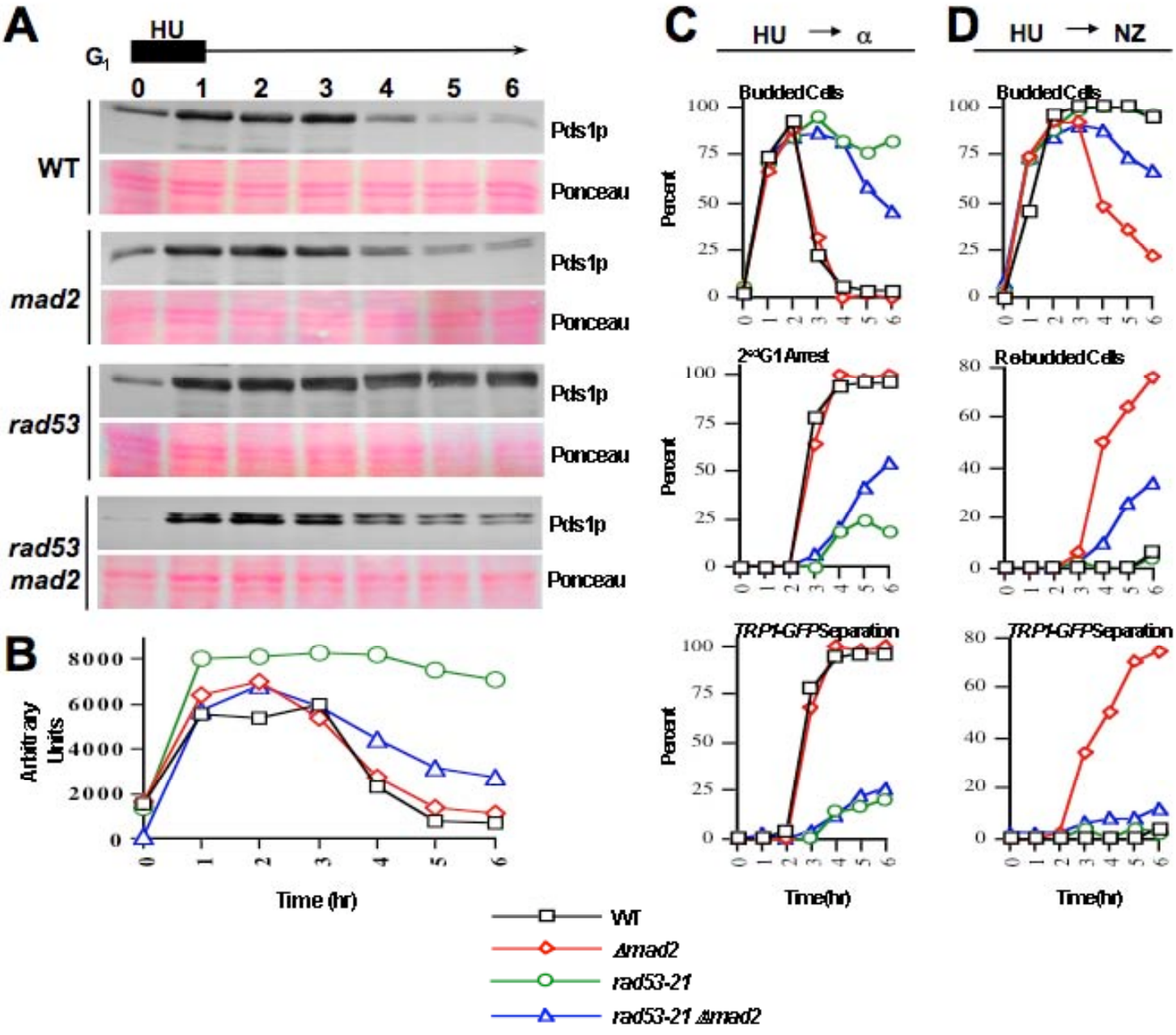

FIGURE S5.—Mitotic progression in *rad53* and *rad53mad2* mutants during HU recovery. A. WT (JBY649), Δ*mad2* (JBY1703), *rad53-21* (JBY1701) and *rad53-21*Δ*mad2* (JBY1705) strains harboring Pds1-Myc were released from G1 into YPD containing 200 mM HU at 30°C for 1 hr. Cells were then washed into fresh YPD pH 3.9 media lacking HU. Mating pheromone was added to restore G1 arrest following completion of mitosis. Protein samples were prepared at the indicated times and processed for Pds1-Myc immunoblotting. Ponceau staining was used to evaluate equivalency of protein load. B. Densitometry analysis of Pds1-Myc immunoblots shown in A. C. WT (JBY1707), Δ*mad2* (JBY1714), *rad53-21* (JBY444), *rad53-21*Δ*mad2* (JBY1718) strains harboring *TRP1-GFP* were treated with 200 mM HU and allowed to recover as in A. Sister chromatid separation was evaluated by scoring the percentage of cells with two distinct GFP foci. D. *TRP1-GFP* separation at was scored as in C., but in this case cells were allowed to recover in YPD media supplemented with 15 mg/ml nocodazole.

File S1

Supplemental Discussion

The unique response of the *rad53* mutant to HU provides us with the opportunity to consider the following questions. First, if centromeres are not replicated in *rad53* cells during HU treatment (resulting in the lack of tension on the spindles), why is the spindle checkpoint not activated to prevent chromosome partition? It has been shown that *cdc6* cells proceed with a reductional mitosis despite the complete absence of replication (Piatti et al., 1995). Similarly, certain alleles of *cdc7* and *dbf4* mutants--encoding the catalytic and regulatory subunits, respectively, of the DDK (Dbf4-dependent kinase), an S phase promoting kinase important for the initiation of DNA replication--were also shown to execute the division of their chromatin when the initiation of DNA replication is blocked (Toyn et al., 1995). These results suggest that the signal that elicits the checkpoint response to inhibit nuclear division may require the establishment of replication forks (Piatti et al., 1995). However, in a population of *rad53* cells in HU, most if not all origins have established a fork (as evidenced by the accumulation of stable stretches of ssDNA). Why, then, can't *rad53* cells activate the spindle checkpoint to inhibit anaphase entry in the presence of HU? Two recent studies have provided clues to this question. Bachant et al. produced compelling evidence that the premature spindle extension and nuclear division in *rad53* cells upon exposure to HU is not through the execution of a true anaphase entry: many of the events associated with anaphase initiation were not observed in *rad53* cells in HU (Bachant et al., 2005). This result was corroborated by a concurrent study where *mec1* cells were also found to initiate chromosome segregation without anaphase entry in the presence of HU (Krishnan et al., 2004). Therefore, chromosome partitioning in *mec1* and *rad53* cells is not a true anaphase and the spindle checkpoint inhibition may not be able to intercede. It is also possible that the activation of a spindle checkpoint may require the localization of Ipl1 protein to the freshly duplicated kinetochores. Therefore, when centromere and kinetochore duplication is absent, Ipl1 may not be recruited to activate the spindle checkpoint.

Second, if *rad53* cells can resume replication after HU removal, why are they unable to achieve bipolar attachment and produce viable offspring? We propose that there exists a small window of time in early S phase for chromosomes to replicate their centromeres and achieve bipolar attachment. Moreover, in *rad53* cells, the lack of early centromere replication in HU also precludes subsequent bipolar attachment of the chromosomes after HU is removed and centromeres replicated, possibly due to structural defects associated with the centromeres/kinetochores or sister chromatid disjunction. Nevertheless, we hypothesize that if premature spindle elongation takes place before centromere duplication, bipolar attachment is inefficient. This hypothesis is consistent with a previously proposed model in which kinetochore attachment to spindle poles requires dynamic searching by the microtubules in three dimensional space before being captured by the kinetchores (Mitchison and Kirschner, 1985). An alternative possibility is that the microtubule dynamics may be attenuated in *rad53* cells, making it difficult for the microtubules to capture the kinetochores. In fact, it has been reported that microtubule associated proteins Cin8 and Stu2 are inappropriately

up-regulated in *mec1* mutant, leading to the unscheduled spindle elongation in the presence of HU (Krishnan et al., 2004). It would be interesting to determine whether the same mechanistic alterations in microtubule dynamics also occur in *rad53* cells. It is also formally possible that the spindle in *rad53* cells in HU suffers damage to the point of irreversible collapse so that even after HU is removed it can no longer be reestablished. However, though we have not directly investigated this possibility, previous studies have shown that the spindles formed in either *rad53* cells in HU or in *cdc6* cells showed rather normal morphology (Bachant et al., 2005; Tanaka et al., 2002).

Our investigation of cell death in *mec1* cells also led to more questions. First, why do *mec1* chromosomes break predominantly during recovery from HU rather than during exposure to HU? It is possible that chromosome breakage due to persistent tension on the spindle is a time-dependent event. For example, *mec1* cells exposed to HU for a prolonged time (up to 3 hrs) also showed increased level of breakage compared to at 1 hr (Fig. 4A), although it is not until HU was removed that the cells displayed drastically more chromosome breakage. It could well be that it is the very act of DNA replication (during the recovery) that facilitates the transition of ssDNA strand breaks into chromosome breakage. The finding of B1 is consistent with our hypothesis that the pericentric region is fragile due to persistent spindle tension. However, it is intriguing that the breakage at this site is only apparent during recovery from, but not during exposure to HU (Fig. 4D). This observation could be explained by two mutually non-exclusive explanations. One, chromosome breakage is facilitated by replication resumption after HU was removed. Two, the level of tension on the spindle might be higher after HU was removed than when it was present. In contrast, B2 was observed even during exposure to HU but increased in frequency during recovery, suggesting that it might occur through a different mechanism from the likely tension-induced break at B1. This observation is consistent with the previous observation that nocodazole treatment does not eliminate all chromosome breaks and supports the notion that there might be breakage that arises independently of tension. Incidentally, B2 is located between two of the most efficient origins on Chr II, *ARS208* and *ARS209* (Fig. 4C). It is possible that when replication forks from these two origins stall as a result of exposure to HU, the stalling forks also prevent other incoming forks to traverse through and replicate the intervening region, which then becomes persistently under-replicated and ultimately leads to chromosome breakage.

Second, is the breakage near the centromere a direct consequence of applied force on the chromosome by the spindle that generates breakage of the phosphodiester bonds? Based on previous calculations of maximum force on a yeast kinetochore microtubule—47 pN (piconewton) measured in the grasshopper spermatocytes (Nicklas, 1983) and 10 pN in budding yeast (Bloom, 2008)—it is unlikely that the force from a pair of microtubules per yeast chromosome (10 pN x 2 microtubules = 20 pN) is enough to break the chromosome, which requires a calculated force of 480 pN (+/-20%) (Bensimon et al., 1995). However, the estimated force for chromosome breakage was calculated for the breaking of double-stranded DNA (Jannink et al., 1996). In the case of *mec1* cells treated with HU, we note that there is ample amount of ssDNA in the pericentric region as well as other parts of

the chromosome. Therefore, chromosome breakage in these cells should require, in theory, less than half of the force to break dsDNA, thus placing the spindle force-induced breakage in the realm of possibility. It warrants further biophysical investigation into the question whether force on the yeast spindle is able to break chromosomes. Nevertheless, we do not posit that the chromosome breakage in *mec1* cells is a direct consequence of the spindle force. In fact, we favor the hypothesis that the spindle force serves to unravel the chromatin such that it might allow nucleases to cleave the DNA at the centromeric regions based on the observation that the two break sites detected near CEN2 in *mec1* cells were very specific, appearing as discrete bands in the agarose gel (Fig. 4D). We have verified these breakage sites using other probes on the *Pst*I fragment (data not shown) and in all instances these sites proved very specific, suggesting an enzymatic action as opposed to mechanical rupture. But we emphasize that the action of nucleases is facilitated by the spindle force to present the substrate (the chromosomes). Recently it has been reported that fission yeast Mus81 cleaves DNA at stalled replication forks after HU treatment in the absence of a replication checkpoint (Froget et al., 2008). It would be interesting to determine whether the budding yeast Mus81 also participates in such an action at the stalled replication forks. We also cannot rule out the possibility that the cleavage furrow during cytokinesis causes the chromosome breakage seen in *mec1* cells and we are in the process of testing this hypothesis. However, once again, the discrete nature of the breakage would argue against such a postulate.

Finally, it is interesting that the more extensive fork progression in HU in *mec1* cells was accompanied by more compromised resumption of fork movement after HU removal. In contrast, *rad53* cells, while unable to replicate centromeres in HU, were more capable of resuming DNA synthesis later. We hypothesize that this difference between *mec1* and *rad53* cells may reflect differences in the regulation of replication fork components by these two kinases in response to replication impediment. It is possible that *mec1* cells specifically lack a critical component restraining fork progression that is important for subsequent fork resumption. We plan to determine whether there exists such a component of the replisome that is specifically subject to regulation by Mec1 but not or to a lesser degree by Rad53 during exposure to HU. Further investigation of what molecular events take place at the replication forks during HU treatment in these two mutants would no doubt aid our understanding of how genome integrity is monitored by the replication checkpoint.

Alvino, G. M., Collingwood, D., Murphy, J. M., Delrow, J., Brewer, B. J., and Raghuraman, M. K. (2007). Replication in hydroxyurea: it's a matter of time. Mol Cell Biol *27*, 6396-6406.

Bachant, J., Jessen, S. R., Kavanaugh, S. E., and Fielding, C. S. (2005). The yeast S phase checkpoint enables replicating chromosomes to bi-orient and restrain spindle extension during S phase distress. J Cell Biol *168*, 999-1012.

Bensimon, D., Simon, A. J., Croquette, V. V., and Bensimon, A. (1995). Stretching DNA with a receding meniscus: Experiments and models. Phys Rev Lett *74*, 4754-4757.

Bloom, K. S. (2008). Beyond the code: the mechanical properties of DNA as they relate to mitosis. Chromosoma *117*, 103-110.

Feng, W., Raghuraman, M. K., and Brewer, B. J. (2007). Mapping yeast origins of replication via single-stranded DNA detection. Methods *41*, 151-157.

Froget, B., Blaisonneau, J., Lambert, S., and Baldacci, G. (2008). Cleavage of stalled forks by fission yeast Mus81/Eme1 in absence of DNA replication checkpoint. Mol Biol Cell *19*, 445-456.

Jannink, G., Duplantier, B., and Sikorav, J. L. (1996). Forces on chromosomal DNA during anaphase. Biophys J *71*, 451-465.

Krishnan, V., Nirantar, S., Crasta, K., Cheng, A. Y., and Surana, U. (2004). DNA replication checkpoint prevents precocious chromosome segregation by regulating spindle behavior. Mol Cell *16*, 687-700.

Mitchison, T. J., and Kirschner, M. W. (1985). Properties of the kinetochore in vitro. II. Microtubule capture and ATP-dependent translocation. J Cell Biol *101*, 766-777.

Nicklas, R. B. (1983). Measurements of the force produced by the mitotic spindle in anaphase. J Cell Biol *97*, 542-548.

Piatti, S., Lengauer, C., and Nasmyth, K. (1995). Cdc6 is an unstable protein whose de novo synthesis in G1 is important for the onset of S phase and for preventing a 'reductional' anaphase in the budding yeast Saccharomyces cerevisiae. Embo J *14*, 3788-3799.

Raghuraman, M. K., Winzeler, E. A., Collingwood, D., Hunt, S., Wodicka, L., Conway, A., Lockhart, D. J., Davis, R. W., Brewer, B. J., and Fangman, W. L. (2001). Replication dynamics of the yeast genome. Science *294*, 115-121.

Tanaka, T. U., Rachidi, N., Janke, C., Pereira, G., Galova, M., Schiebel, E., Stark, M. J., and Nasmyth, K. (2002). Evidence that the Ipl1-Sli15 (Aurora kinase-INCENP) complex promotes chromosome bi-orientation by altering kinetochore-spindle pole connections. Cell *108*, 317-329.

Toyn, J. H., Johnson, A. L., and Johnston, L. H. (1995). Segregation of unreplicated chromosomes in Saccharomyces cerevisiae reveals a novel G1/M-phase checkpoint. Mol Cell Biol *15*, 5312-5321.

FILE S2

Supplemental Experimental Procedures

Microarray hybridization and analysis

The HH and HL DNA for each timed sample from the density transfer experiments were mixed for co-hybridization and likewise, the ssDNA-labeled S phase and G1 control samples from the ssDNA mapping experiments were also mixed for co-hybridization to DNA microarrays (Agilent G4140A) according to the manufacturer's recommendations. The algorithms used for analyzing microarray data have been described previously (Alvino et al., 2007; Feng et al., 2007) except that a Lowess smoothing algorithm instead of Fourier transformation was applied in the current study to avoid an artifact introduced by the latter at the telomeric regions of a chromosome. Microarray data were processed and analyzed as follows:

1. The output files following Agilent slide scanning and data extraction are edited to remove data corresponding to array spots flagged by the software as anomalous. Spots corresponding to known sequence repeats are also eliminated. The edited data are referred to as "Raw data".

2. Raw data are normalized using the scheme described previously (Alvino et al., 2007). This routine requires input of either one or two experimentally determined parameters, depending on the type of experiment (%HL vs. ssDNA).

3. Normalized data are smoothed using a Lowess smoothing algorithm. First, a window size **w** is specified for the overall smoothing of the profile. The "coordinate set" for a given chromosome is the collection of probe coordinates on the array that lie on that chromosome. For each coordinate **t** in the coordinate set, consider the interval **I(t)=(t-w/2, t+w/2)**. Next, determine the set of all locations in the coordinate set that lie in this interval **I(t)** and do a weighted regression on the associated data points using the weight function:

$$\mathbf{wtfunc}[x-t, w] = \left(1 - \frac{8 * \mathbf{Abs}(-t+x)^3}{w^3}\right)^3$$

on the interval **I(t)**. In this way, for each **t** in the coordinate set we obtain a value **L(t,w)**. The new data set of pairs (**t, L(t,w)**) is the Lowess smoothed profile for the given chromosome.

4. Extrema (local maxima and minima) are determined as in (Raghuraman et al., 2001) for the output of either smoothing method.

TABLE S1

The distance between centromeres and their closest potential origin of replication (ARS)

Centromere	CEN coordinate (bp)	nearest ARS to CEN	Checked?	ARS coordinate (bp)	Dis. (CEN-ARS) (bp)
CEN1	151526	ARS108	No	147197	4329
CEN2	238267	ARS208	No	237762	505
CEN3	114441	ARS308	N/A	114624	183
CEN4	449763	ARS416	No	462565	12802
CEN5	152045	ARS510	No	145661	6384
CEN6	148565	ARS605	No	136030	12535
CEN7	496983	ARS719	No	485046	11937
CEN8	105640	Likely ARS	No	111335	5695
CEN9	355684	ARS920	No	357275	1591
CEN10	436360	ARS1015	No	442453	6093
CEN11	439831	ARS1114	No	447775	7944
CEN12	150887	ARS1208	N/A	151168	281
CEN13	268090	ARS1309	No	263179	4911
CEN14	628819	ARS1426	No	635781	6962
CEN15	326644	ARS1513	No	337404	10760
CEN16	556012	Likely ARS	Yes	559633	3621

Centromere coordinates were obtained from the *Saccharomyces cerevisiae Genome Database* (http://yeastgenome.org) and the mid point of each centromere (column 2) was calculated. The identities of the nearest potential origin to each centromere (column 3) were obtained from oriDB (http://www.oridb.org) compiled by Conrad Nieduczynski and the mid point of each ARS (column 4) was calculated. The distance between the midpoint of a centromere and that of its nearest ARS is reported in column 5.

TABLE S2

Yeast strains used in this study

Name	Genotype	Background	Source
HM14-3a	*MATa bar1-1 his6 leu2-3,112 trp1-289*	A364a	Feng et al., 2006
WFY34	*MATa rad53::rad53K227A(KanMX4) bar1-1 his6 leu2-3,112 trp1-289*	A364a	Feng et al., 2006
yMP10913	*MATa mec1-1 sml1 ade2 ade3 leu2 trp1 ura3 SLR::URA3*	A364a	B. Garvik
BY2226	*MATa mec1-1::HIS3 sml1-1 his3 leu2 trp1 ura3*	A364a	L. Breeden
WFY32	*MATa bar1-1 his6 leu2-3,112 trp1-289 ura3-52 pRS315 pRS316*	A364a	This study
WFY71	*MATa rad53::rad53K227A(KanMX4) bar1-1 his6 leu2-3,112 trp1-289 ura3-52 pRS315 pRS316*	A364a	This study
WFY73	*MATa mec1-1::HIS3 his3 leu2 trp1 ura3::URA3*	A364a	This study
SBY1	*MATa ura3-1 leu2-3,112 his3-11 trp1-1 can1-100 ade2-1*	W303	S. Biggins
WFY88	*MATa rad53::rad53K227A(KanMX4) ura3-1 leu2-3,112 his3-11 trp1-1 can1-100 ade2-1*	W303	This study
SBY630	*MATa ipl1-321 ura3-1 leu2-3,112 his3-11 trp1-1 can1-100 ade2-1*	W303	S. Biggins
WFY81	*MATa ipl1-321 rad53::rad53K227A(KanMX4) ura3-1 leu2-3,112 his3-11 trp1-1 can1-100 ade2-1*	W303	This study
SBY292	*MATa mad2::URA3 ura3-1 leu2-3,112 his3-11 trp1-1 can1-100 ade2-1*	W303	S. Biggins
WFY89	*MATa mad2::URA3 rad53::rad53K227A(KanMX4) ura3-1 leu2-3,112 his3-11 trp1-1 can1-100 ade2-1*	W303	This study
JBY686	*MATa cdc23-1 CEN4-lacO-LEU2 his3-11,15-lacI-GFP-HIS3 leu2-3,112 trp1-1, ura3-1 ade2-1 can1-100*	CRY	This study
JBY1720	*MATa cdc23-1 Δmec1::HIS3 CEN4-lacO-LEU2 his3-11,15-lacI-GFP-HIS3 leu2-3,112-GAP-RNR3-LEU2 CEN4-GFP trp1-1, ura3-1 ade2-1 can1-100*	CRY	This study
JBY1726	*MATa cdc23-1 CEN4-lacO-LEU2 his3-11,15-lacI-GFP-HIS3 leu2-3,112 trp1-1, ura3-1 ade2-1 can1-100*	CRY	This study
JBY1728	*MATa cdc23-1 rad53K227A-KanMX CEN4-lacO-LEU2 his3-11,15-lacI-GFP-HIS3 leu2-3,112 trp1-1, ura3-1 ade2-1 can1-100*	CRY	This study
JBY1729	*MATa cdc23-1 rad53K227A-KanMX CEN4-lacO-LEU2 his3-11,15-lacI-GFP-HIS3 leu2-3,112 trp1-1, ura3-1 ade2-1 can1-100*	CRY	This study
JBY1732	*MATa cdc23-1 CEN4-lacO-LEU2 his3-11,15-lacI-GFP-HIS3 PDS1-HA-URA3 leu2-3,112 trp1-1, ura3-1 ade2-1 can1-100*	CRY	This study
JBY1735	*MATa cdc23-1 rad53-21 CEN4-lacO-LEU2 his3-11,15-lacI-GFP-HIS3 PDS1-HA-URA3 leu2-3,112 trp1-1, ura3-1 ade2-1 can1-100*	CRY	This study
JBY1736	*MATa cdc23-1 rad53-21 CEN4-lacO-LEU2 his3-11,15-lacI-GFP-HIS3*	CRY	This study

	PDS1-HA-URA3 leu2-3,112 trp1-1, ura3-1 ade2-1 can1-100		
JBY649	*MATa PDS1-Myc-LEU2 his3-11,15 leu2-3,112 trp1-1, ura3-1 ade2-1 can1-100*	CRY	This study
JBY1703	*MATa Δmad2::URA3 PDS1-Myc-LEU2 his3-11,15-lacI-GFP-HIS3 leu2-3,112 trp1-1, ura3-1 ade2-1 can1-100*	CRY	This study
JBY1701	*MATa rad53-21 PDS1-Myc-LEU2 his3-11,15-lacI-GFP-HIS3 leu2-3,112 trp1-1, ura3-1 ade2-1 can1-100*	CRY	This study
JBY1705	*MATa rad53-21 Δmad2::URA3 PDS1-Myc-LEU2 his3-11,15-lacI-GFP-HIS3 leu2-3,112 trp1-1, ura3-1 ade2-1 can1-100*	CRY	This study
JBY1707	*MATa trp1-1-lacO-TRP1-LEU2 his3-11,15-lacI-GFP-HIS3 leu2-3,112 ura3-1 ade2-1 can1-100*	CRY	This study
JBY1714	*MATa Δmad2::URA3 trp1-1-lacO-TRP1-LEU2 his3-11,15-lacI-GFP-HIS3 leu2-3,112 ura3-1 ade2-1 can1-100*	CRY	This study
JBY444	*MATa rad53-21 trp1-1-lacO-TRP1-LEU2 his3-11,15-lacI-GFP-HIS3 leu2-3,112 ura3-1 ade2-1 can1-100*	CRY	This study
JBY1718	*MATa rad53-21 Δmad2::URA3 trp1-1-lacO-TRP1-LEU2 his3-11,15-lacI-GFP-HIS3 leu2-3,112 ura3-1 ade2-1 can1-100*	CRY	This study

Those strains with a CRY background were derived from W303 background as previously described (Bachant et al., 2005).